Heliyon 10 (2024) e33272

Contents lists available at ScienceDirect

Heliyon

journal homepage: www.cell.com/heliyon

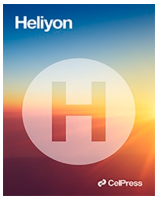

Review article

Recent advances in the metamaterial and metasurface-based biosensor in the gigahertz, terahertz, and optical frequency domains

Shadmani Shamim, Abu S.M. Mohsin *, Md. Mosaddequr Rahman, Mohammed Belal Hossain Bhuian

Department of Electrical and Electronic Engineering, Optics and Photonics Research Group, BRAC University, Kha 224 Bir Uttam Rafiqul Islam Avenue, Merul Badda, Dhaka 1212, Bangladesh

ARTICLE INFO

Keywords:
Metamaterials
Metasurface
Frequency domain
Sensor configuration
Biosensing

ABSTRACT

Recently, metamaterials and metasurface have gained rapidly increasing attention from researchers due to their extraordinary optical and electrical properties. Metamaterials are described as artificially defined periodic structures exhibiting negative permittivity and permeability simultaneously. Whereas metasurfaces are the 2D analogue of metamaterials in the sense that they have a small but not insignificant depth. Because of their high optical confinement and adjustable optical resonances, these artificially engineered materials appear as a viable photonic platform for biosensing applications. This review paper discusses the recent development of metamaterial and metasurface in biosensing applications based on the gigahertz, terahertz, and optical frequency domains encompassing the whole electromagnetic spectrum. Overlapping features such as material selection, structure, and physical mechanisms were considered during the classification of our biosensing applications. Metamaterials and metasurfaces working in the GHz range provide prospects for better sensing of biological samples, THz frequencies, falling between GHz and optical frequencies, provide unique characteristics for biosensing permitting the exact characterization of molecular vibrations, with an emphasis on molecular identification, label-free analysis, and imaging of biological materials. Optical frequencies on the other hand cover the visible and near-infrared regions, allowing fine regulation of light-matter interactions enabling metamaterials and metasurfaces to offer excellent sensitivity and specificity in biosensing. The outcome of the sensor's sensitivity to an electric or magnetic field and the resonance frequency are, in theory, determined by the frequency domain and features. Finally, the challenges and possible future perspectives in biosensing application areas have been presented that use metamaterials and metasurfaces across diverse frequency domains to improve sensitivity, specificity, and selectivity in biosensing applications.

1. Introduction

The successful application of light control in which light and other energy forms act naturally and are managed in a controlled way has given rise to the metamaterials field in the material science domain, which is currently in development. Physics, chemistry,

* Corresponding author.
E-mail address: asm.mohsin@bracu.ac.bd (A.S.M. Mohsin).

https://doi.org/10.1016/j.heliyon.2024.e33272
Received 13 March 2024; Received in revised form 17 June 2024; Accepted 18 June 2024
Available online 21 June 2024

material science, and engineering can all be correlated thanks to metamaterials, which are defined as artificial composite structures with distinctive material properties.

The work on artificial materials by Pendry, Smith et al., and others introduced novel properties like a negative refractive index and a near-zero index [1]. These man-made substances are commonly referred to as metamaterials because they each have a resonant scatterer. A brief introduction to such metamaterials and their 2D counterparts, known as metasurfaces, serves as the introduction to this review. Analytically, the expansion of Floquet modes explains the properties of metamaterials and metasurfaces by illuminating their emission behavior and quantum emission [2,3]. Floquet modes with higher propagating orders need to be acknowledged for the accurate representation of such structures when the periodicity of the individual scatterers of these artificial materials approaches close concerns for the wavelength in operation. As per scattering theory, all scattering objects can be equivalent to effective electric and/or magnetic polarizability densities. These electric and magnetic resonance modes are supported in dielectric materials. For a single resonant structure (rectangular, spherical, and water-droplet configuration), the magnetic resonances are stronger than the electronic resonances, enabling ultra-broadband absorption after optimization [4]. These structures are not categorized as metamaterials or metasurfaces. Therefore, research is still ongoing in the vast field of metamaterials and metasurface. Consequently, the evaluation won't be very thorough. However, the main research in the biosensing field, as well as pertinent literature, is presented in this paper.

1.1. Metamaterials

Electric and magnetic dipole moments are formed when an electromagnetic wave interacts with a composite material. These moments are inextricably linked to the effective permittivity and permeability of the material. Changing the medium's size, shape, orientation, and density makes it possible to produce materials with specific electromagnetic responses. Metamaterials are one category of synthetic material. Depending on which specific elements are resonant, these materials may exhibit negative permittivity and permeability values. Because resonances have the property that their phase response reverses as frequency changes around resonance, only resonant individual elements can display negative refractive index features [5]. In the literature, these items are referred to as left-handed media and backward-wave media [6,7].

The magnetic properties of metamaterials can be explained using the Lorentz classical theory, which asserts that the electron is viewed as a damped harmonic oscillator in an electromagnetic field [8,9]. When the restoring force is negligible, the Drude model takes the role of the Lorentz model. The Drude Model yields negative permittivity and permeability values over a large frequency range [9].

In metamaterials with resonant individual elements, the relative permittivity and permeability values can be negative. These refractory materials diminish the refracted angle, allowing the incident and refracted waves to collide (negative refraction), causing the refracted wave to lay on the opposite side of the normal wave. Because of this negative refractive phenomenon, electromagnetic waves, including light, can be completely controlled in all four quadrants of the cartesian plane. Because of this unique characteristic, metamaterials can be employed in ways that natural materials cannot [9].

A near-zero refractive index is another characteristic of metamaterials that is absent from natural materials. Such materials have either a permittivity or permeability real part that is almost at zero refractive indexes (both the permittivity and permeability have real parts that are almost zero). At frequencies spanning from low microwaves to optical, these metamaterials offer a wide range of possible electromagnetic applications, including but not limited to antennas, electronic switches, shielding, novel substrates, "perfect lenses," and more [2].

Vaselago's theoretical work on metamaterials served as the foundation for early research [10], and Pendry, Smith et al. implemented it [1]. Such materials have been around for over a century. Sivukhin gave a brief overview of the characteristics of metamaterials in 1957 [11]. Malyuzhinets [12] and Silin [13–15] made references to L. I Mandel'shtam. The 1904 paper by Lamb was cited by Mandel'shtam himself in Refs. [16,17]. Lamb was the first to propose backward waves existence or waves with group velocities and opposing phases [18]. Along with briefly mentioning Lamb's work, Schuster also provided an optical refraction realization after locating a medium with backward-wave characteristics [19]. A similar backward wave formation was demonstrated in Pocklington in 1905 using a bicycle chain suspended in a specific manner [20]. In theory, early metamaterials research primarily concentrated on the creation of artificial magnetism in the microwave region, negative refractive index, negative refraction, and superlens [21]. Nevertheless, as time went on, terahertz and optical frequencies became the focus of metamaterials research. Since then, new metamaterial-based device prototypes and fields of material research have emerged.

1.2. Metasurfaces

Metasurfaces are the 2D counterpart/surface counterpart of metamaterials, to put it simply. Like metamaterials, the response of metasurfaces can be described by their electric and magnetic polarizabilities. These metasurfaces' permittivity and permeability values are used in some literature to categorize them as metafilms. Even though electromagnetic waves are manipulated using the propagation effect, metamaterials can control the movement of light. A structure with a fair amount of bulk may be produced by this process. Metasurfaces, on the other hand, can control the wave over a single, incredibly thin layer [22,23]. Because of the 3D nature of metamaterials' planar structure and the difficulty of fabricating using planar fabrication tools, this is also a drawback. Additionally, this planar fabrication method is less expensive than the intricate production of 3D metamaterials [24,25]. Because they are a 2D material, metasurfaces are simple to incorporate into other devices and maintain a smaller overall size and lower risk of loss [2,26–28].

Broadband metasurface filters can be created using this technology. To manage these dispersion characteristics, the primary and

secondary magnetic resonances, and plasma wavelengths for permittivity, were altered. These features are determined via the construction and optimization of sub-wavelength deep notches using a genetic algorithm. Furthermore, broadband metasurfaces have a low transmission band insertion loss [29].

The geometrical parameters of the meta-atoms, which make up metamaterials and metasurfaces, are used to describe their optical properties. These meta-atoms are made up of one or more high-index dielectrics or noble metals nanostructures that are smaller than a wavelength [30]. Following the creation of the first artificial materials, metamaterials showed a variety of uses, including superlens, nearly perfect absorption, transmission, and metamaterials with negative refractive index [30]. Subsequently, metasurfaces took the place of metamaterials to produce even more novel functionalities, such as planar lenses, the ultrathin invisibility cloak, and the generalization of Snell's law [1,31,32].

Sub-wavelength thickness-based planar metamaterials and metasurfaces can be fabricated through nanoimprinting and lithography. Metasurfaces can offer the same phenomena as metamaterials except for having negligible loss, a theoretically straightforward realization, and an easier fabrication process. Metasurfaces can modify the wavefront of light via the change of phase in an abrupt manner [30].

One of the most significant uses of metamaterials, in addition to the superlens and slow-light cloaking, is lab-on-chip photonics refractive index (RI) biosensing. A change in the refractive index can be seen through biomolecular interaction layers in various analyte layers. Electromagnetic (EM) RI has unique properties for sensitive and label-free biochemical assays in several biological and chemical sensing applications. The meta-atoms and their configurations can change the resonant EM spectrum, which is significantly influenced by its surroundings. Measuring the RI of the nearby biomolecular analyte is possible [30]. Additionally, due to their signal stability and tolerance, sensors based on metamaterials and metasurfaces have many advantages over conventional surface plasmon polariton (SPP) based sensing platforms. A higher quality factor and lower radiative damping caused by plasmonically induced transparency or Fano-resonance are two additional benefits of periodic meta-atoms [33,34]. A unit cell or supercell made up of several meta-atoms can have a variety of resonances and slow light effects. In SPP biosensors, these results are challenging to achieve [30].

This paper presents an overview of recent developments in a variety of biosensing applications based on metamaterials and metasurfaces. The unique value of this article is that it covers various aspects of metamaterials and metasurfaces' biosensing applications. The main classification of the sensing is based on the frequency domains of the electromagnetic spectrum (gigahertz, terahertz and optical), however, various other parameters such as material selection, resonant mechanism, and topologies were included in the organization, providing a broader perspective and various scopes of research for readers, especially the new ones.

2. Performance evaluation parameters of biosensing applications

Biosensors are essential in many fields such as health care and disease detection, food and water safety, drug delivery, and environmental monitoring, and can be viewed as important tools for biological phenomena investigation. A biosensor is an integrated receptor-transducer-based device that converts the biological response to an electrical signal [35,36]. The main challenges with the advancement of biosensors are efficiency which means the capture of biorecognition signals and conversion of these signals to electrical responses, improvement of sensor performance meaning improved sensitivity, faster response time, reproducibility, and low detection limit, and finally the miniaturization of biosensing devices with the help of micro and nano-manufacturing techniques [36]. Fluorescence-based methods have proven useful for both genomic and proteome microarray analysis [37,38] and imaging, including single-molecule detection in living cells [39,40]. However, the fluorescence-based methods can be expensive and time-consuming and based on the application, this may not be possible. Furthermore, biological reactions generally rely on biomolecules having three-dimensional structures, which can be manipulated by the addition of fluorescent labels. Therefore, bioanalytical sensing technologies that can directly detect target molecules without labeling are imperative [35].

Various parameters are used for the evaluation and comparison of the biosensor performance. These parameters are sensitivity, the figure of merit (FOM), the Q factor, the limit of detection (LoD), and specificity/selectivity [36,41]. Sensitivity (S) or RI sensitivity is defined as the ratio of the sensor output change. For example, the change in wavelength shifts $\Delta\lambda$ to the change in refractive index Δn. Another important characteristic is the FOM. It is typically expressed as FOM=S/FWHM, where S is the sensitivity and FWHM is the full width at half maximum resonance. This parameter is used to design and optimize nanostructures for biosensor development. The smallest change in the RI is characterized by the figure of merit. The Q factor is another widely used parameter. Q factor reflects the resonance characteristics, expressed as $Q = \lambda_r/(\text{FWHM})$, where λ_r is the resonance wavelength [41]. LoD is a common characteristic of biosensor performance, which is a measurement of the smallest detectable concentration of the analyte in a biosensor. According to the IUPAC (International Union of Pure and Applied Chemistry), LoD is defined "as analyte concentration that produces a response as $R_{LoD} = R_B + 3\sigma_{RB}$; R_B is mean and σ_{RB} is the standard deviation of the response to a blank specimen" [42]. The performance of the main components of biosensors, properties of the analyte, and environmental factors affect the limit of detection (LoD) of the biosensors [43]. Specificity/selectivity is another important performance characteristic of a biosensor that detects and characterizes the target analyte in a complex sample without other components' interference [41].

Hence, the metamaterial and metasurface-based biosensing applications are explained in detail as per the classification mentioned in the following sections.

3. Classification of Metamaterials and Metasurfaces in Biosensing Applications

Recently, biosensing technologies based on metamaterials and metasurfaces have received a great deal of attention from microwave to optical frequencies due to their cost-effective and label-free biomolecule detection. Sen et al. and coworkers did a broad review

of optical, radio frequency (RF), microwave, millimeter wave (mmW), and terahertz biosensors [35]. In their work, biomatter and wave interaction modalities were considered over a range of applications. Based on their work, biological tissue was considered a dielectric structure, characterized by frequency-dependent parameters named permittivity and conductivity [35]. For biosensors in the optical frequency domain, the change in permittivity meant a change in the optical properties such as photoluminescence, reflection intensity, reflectance angle, and interference pattern through techniques like surface plasmon resonance (SPR), Surface Enhanced Raman Scattering (SERS), interferometry. On the other hand, for the gigahertz (GHz) domain, changes in permittivity can be reflected as changes in capacitance based on components like resonator (split ring, cavity) and microstrip structures [35]. These structure configurations are modeled in terms of RLC circuits in which the capacitance works as a function of permittivity. As resonators and microstrip structures are part of the oscillator circuit where the resonant frequency changes with the capacitance change, thereby causing a change in the biomolecular concentration. GHz-based frequency domain often utilizes microwave frequencies and therefore these microwave-based biosensors provide high sensitivity, selectivity, and real-time monitoring of biological reactions [35].

Therefore, in this literature, most of the biosensors mentioned were focused on label-free and ex-vivo along with a detailed review of the in-vivo techniques in the GHz and THz domain (Doppler radar, ultra-wideband radar, near field sensing, microwave imaging, wave spectroscopy) and optical frequency domain (optical spectroscopy, backscattering, Laser Doppler blood flow symmetry) [35]. Label-free techniques have an advantage over label-based techniques as the label-based technique can alter the binding properties, thereby introducing systematic error in the sensing analysis. Hence, label-free techniques have an advantage over label-based techniques [35,44].

For biosensing in the optical frequency range, the selection of materials acts as a medium for the generation of surface plasmon resonance and localized surface plasmon resonance. Optimization of material is important for material selection. Optimization is performed based on the carrier concentration, determining the wavelength range where the material is active [45]. Metals contain high carrier concentrations leading to their response in the visible and UV range of the optical range. Whereas low carrier concentration in semiconductors and graphene leads to a response in the IR and THz range [45]. Ohmic losses are dominant in the high frequencies [46]. Therefore, an ideal material will exhibit low optical and ohmic losses and research is currently ongoing for the identification of such materials [47]. In the meantime, common and noble metals such as gold (Au) and silver (Ag) show surface plasmon polariton (SPP) at the visible part of the spectrum. But these materials exhibit different properties in the THz regime making it hard for containment of SPPs at the flat metal inter-surface. THz frequency is far below the metal's plasma frequency. These materials have a very high conductivity resembling a perfect electric conductor (PEC) [47]. The SPP's electric field slightly penetrates the material causing poor confinement. To overcome this poor penetration of THz wave, the metal surfaces are engineered to support the SPP-like modes making metamaterials an excellent example [48]. Graphene is an emerging plasmon material possessing excellent photoelectric properties such as tunability, low losses, tight field localization, and a broad response spectrum [49]. Graphene has a low carrier concentration and is typically active in the THz region. Metamaterials make it possible to detect biomolecules in THz-GHz frequency regimes, which would otherwise be impossible because microorganisms such as viruses, fungi, and bacteria have scattering cross-sectional areas much smaller than terahertz and gigahertz wavelengths [50].

Therefore, in our work, in alignment with the literature [35,51], we will focus on the label-free, ex-vivo measurement technique for GHz, THz, and optical frequency range, focusing on resonator and microstrip structures and physical mechanisms such as localized surface plasmon resonance, Fano-resonance, hyperbolic dispersion, and chirality. As for the selection of materials, we have narrowed down the materials to noble metals (Au, Ag, Cu, Al), two-dimensional (2D) materials (graphene, carbon nanotube, black phosphorous), dielectric (Silicon), and hybrid metamaterials. Based on the electromagnetic wave spectrum, the biosensors in our work can be divided according to the frequency domain of the electromagnetic (EM) spectrum into gigahertz domain (RF, microwave, and millimeter wave), terahertz domain (THz), and optical frequency domain.

One of the most critical characteristics in determining the performance of biosensing applications is sensitivity. The sensitivity is dependent upon the optimization of the structural topology of the metamaterials and their constituent material selection. Most publications in this area have worked on structure topology optimization rather than material selection. One of the primary reasons could be that the field of metamaterials has undergone a transitional stage in which design theories and practical applications facilitated the appropriate constituent material selection. Therefore, the design of suitable metamaterials for highly sensitive sensing for the THz region necessitates the practical applications in which the materials' properties play an important role. Therefore, we focus mainly on the constituent material selection part along with highlighting the advances in biosensing applications in the THz region [51]. Although the importance of constituent materials lies in the other frequency domains (GHz and optical) and overlaps there also, for our work, we focus on the material selection-based classification for the THz frequency region only, however, the material-selection feature overlaps into the gigahertz and optical frequency domains also.

In terms of the mechanism-based features regarding surface plasmon resonance, Fano-resonance, hyperbolic dispersion, and chirality, we focused on the optical frequency range. SPR is a phenomenon that occurs in the visible to near-infrared spectrum and is related to electron collective oscillations at the interface of a metal and a dielectric medium. However, SPR is not routinely detected in the GHz and THz frequency domains in the same way that it is in the optical range. Therefore, plasmonic components can be included in metamaterials or metasurfaces to improve sensitivity and selectivity for biosensing applications [45,52]. We will focus on this mechanism in the optical frequency domain only for our work.

Due to factors such as sensitivity, size, wavelength scale, losses, and quality factors, as well as device integration and manufacturing issues, Fano resonance is frequently used in biosensing applications in the THz and optical frequency ranges rather than the GHz range. Even tiny changes in refractive index or the presence of molecules can cause considerable variations in the Fano resonance spectrum in the THz and optical regions, where the interaction with matter is often greater. As a result, it is ideal for ultrasensitive biosensing applications. The diameters of the resonant components in the THz and optical bands may be set at subwavelength scales, allowing for

fine control and modulation of the resonance. However, in the GHz range, the size of the resonant components grows equivalent to the wavelength, making subwavelength confinement and control for Fano resonance difficult. Fano resonances are extremely sensitive to losses in the metamaterial structure, which can reduce the resonance's quality factor (Q-factor). Losses are often smaller in the THz and optical frequencies, allowing for greater Q-factors and sharper Fano resonances. Losses are often larger in the GHz range, limiting the potential Q-factors and the quality of the Fano resonance. Fabricating and integrating metamaterial structures at THz and optical frequencies can be difficult, although they are frequently more practicable than in the GHz range. Advanced nanofabrication techniques for THz and optical frequencies are well-established, allowing the production of complicated metamaterial designs. The manufacturing problems in the GHz range are significantly higher, and structures may be constrained to simpler designs, impacting the adaptability and performance of Fano resonances [53].

The manipulation of electromagnetic waves at subwavelength scales is made possible by hyperbolic dispersion, allowing for more control over light-matter interactions. Subwavelength confinement is simpler to achieve in the THz and optical frequencies, where wavelengths are often in the hundreds of nanometers to micrometers range, allowing the design and construction of metamaterial structures with hyperbolic dispersion. Anisotropic optical qualities characterize hyperbolic metamaterials, which means that the refractive index fluctuates with direction. This anisotropy opens new possibilities for adjusting light propagation and modulation, enabling the development of innovative biosensing devices. Because of the longer wavelengths involved, it is often more difficult to obtain substantial anisotropy and control over light propagation in the GHz range. Furthermore, hyperbolic metamaterials can improve light-matter interaction, allowing more sensitive biosensing. Because of the subwavelength confinement and higher density of states associated with hyperbolic dispersion, field localization, and light-matter interaction strengths are improved. This is especially useful in the THz and optical frequencies, where electromagnetic waves interact with biological or chemical analytes more strongly

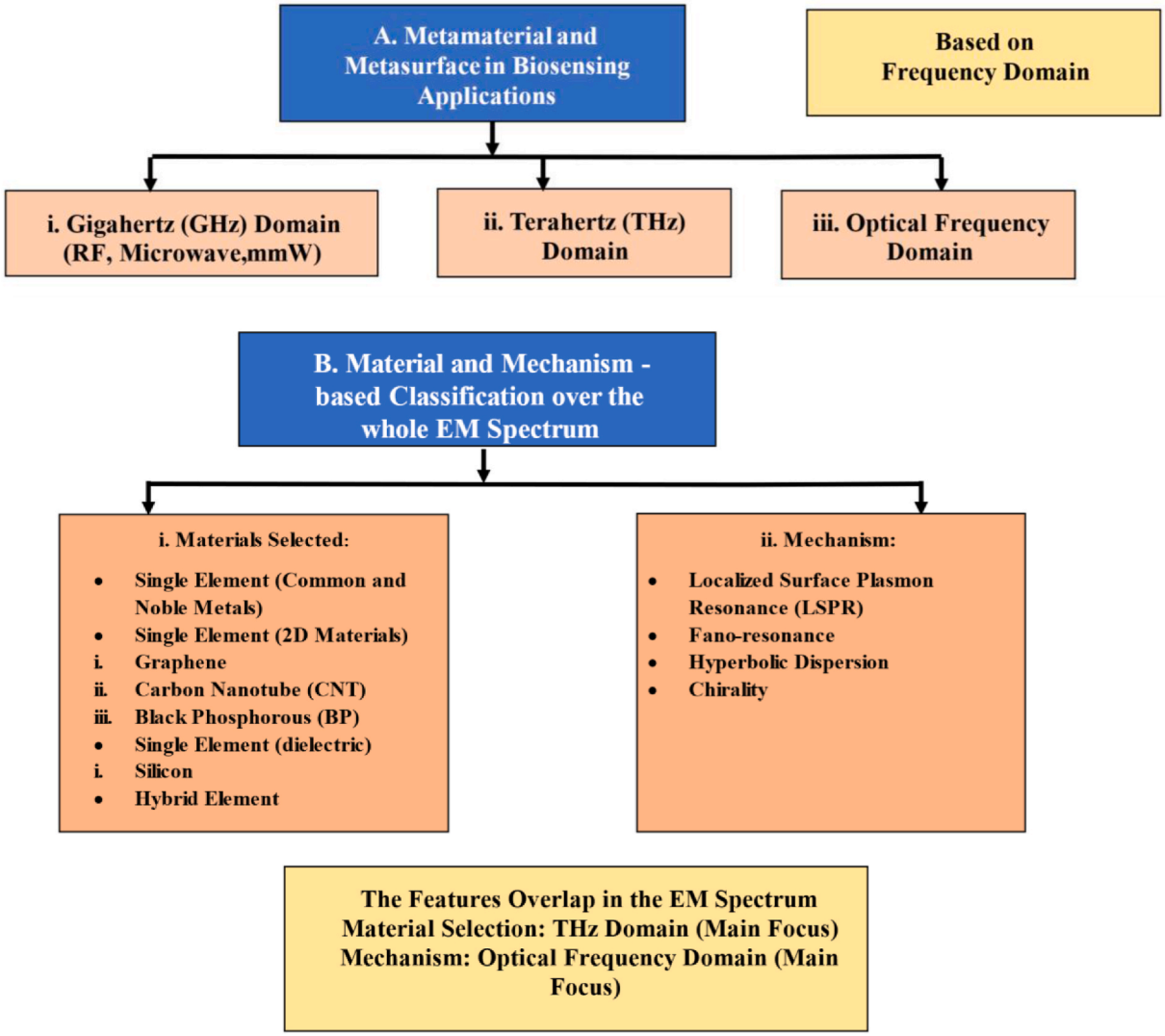

Fig. 1. Classification of Metamaterials and Metasurfaces in Biosensing Applications based on the frequency domains, materials, and mechanism.

than in the GHz region [54–57].

As for chirality, it is a feature that results from the absence of mirror symmetry in a structure, molecule, or substance. Many biological and chemical compounds are chiral in the THz and optical regions. By adding chiral metamaterials into biosensing platforms, it is feasible to selectively interact with and detect the presence of chiral compounds such as amino acids, proteins, carbohydrates, and medicines. As a result, chirality is a crucial tool for detecting and characterizing biomolecular structures and their interactions. Circularly polarized light is abundantly available in the THz and optical frequencies and may be effectively linked with chiral metamaterials to produce unique responses, enabling precise detection and characterization of chiral analytes. Furthermore, chiral metamaterials are frequently composed of subwavelength chiral components with significant chiroptical responses in the THz and optical regimes. The capacity to construct subwavelength structures is critical for obtaining precise control over light-matter interactions. In the GHz region, where the wavelengths are greater, achieving subwavelength confinement and control becomes more difficult, limiting the usefulness of chiral metamaterials for biosensing applications. Also, by modifying the chiral response of metamaterials, it is feasible to increase detection limits and accuracy by increasing the signal-to-noise ratio and discriminating between distinct chiral analytes. This sensitivity and specificity are especially significant in the THz and optical frequencies, where chiral compounds interact with electromagnetic waves more strongly [58,59].

In principle, while these mechanisms are frequently linked with higher-frequency ranges, such as the optical domain, they may also be adapted and used in the GHz frequency range for biosensing applications based on metamaterials and metasurfaces. The design and optimization of certain structures and materials are critical in achieving these effects at lower frequencies. However, for our work, we are focusing on the mechanism-based classification for the optical frequency domain, although the overlap of the mechanism-based features will be seen in the other domains (mainly the THz domain).

A detailed description of the application of metamaterial and metasurface-based biosensing applications based on our classification is depicted in Fig. 1.

3.1. Metamaterial and metasurface-based biosensors in the GHz domain

The radio frequency (RF), microwave, and millimeter wave (mmW) were considered in the GHz frequency domain in our work. Radio waves and microwaves are a form of electromagnetic radiation with operating frequencies ranging from 30 to 300 MHz and 300 MHz to 300 GHz, respectively, whereas millimeter waves lie within the frequency range of 30–300 GHz [60,61]. MEMS technology and photolithography were proposed for metamaterial-based RF biosensors between 2008 and 2012 [50,62–64]. A split-ring resonator (SRR) can be utilized to generate a negative magnetic permeability material in a time-varying H-field component of a perpendicularly polarized wave incident on its surface [65,66].

Metamaterials are described as artificially defined periodic structures exhibiting negative permittivity and permeability simultaneously [1,67]. Properties like shape, orientation, geometry, and a properly excited electric and magnetic field can all affect how a metamaterial behaves. The outcome of the sensor's sensitivity to an electric or magnetic field and the resonance frequency are, in theory, determined by the metamaterials selected [68]. In comparison to substrate-integrated waveguide (SIW) technology [69], circuits based on metamaterials exhibit excellent performance. The electrical length and characteristic impedance are therefore key design factors for metamaterials. Our analysis indicates that, among the metamaterial structures, the split ring resonator (SRR) is the configuration that has received the most research. Negative permeability and negative permittivity are the two most intriguing properties of synthetically created metamaterials. Negative permeability is present in the split ring resonators close to the resonance frequency. A negative permeability is seen when the incident magnetic field is parallel to the split ring resonator's (SRR) plane [49].

The metamaterial biosensors that are based on the popular LC arrangement (split-ring resonator) are based on the design and measurements of metallic layers. The inductance L compares to the continuous metallic parcels, whereas the capacitance C is related to the gap between the metallic layers [70].

Lee et al. [71] were the first to apply metamaterial in biosensing. They demonstrated the metamaterial's biosensing capacity by using a gold split ring resonator (SRR) array to detect biotin and streptavidin. SRR functioned as a biosensor because it is a basic LC circuit with a simple resonance frequency of $f_o = 1/[2\pi(LC)]^{1/2}$ shown in Fig. 2 (Left 2a and Right 2b). The formula stated that the

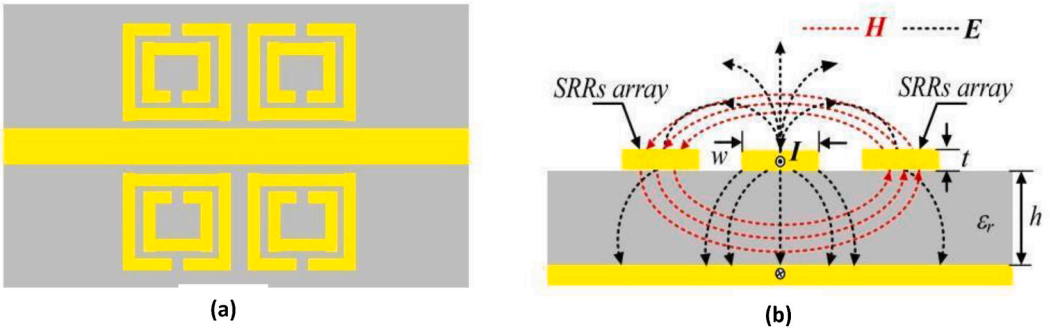

Fig. 2. Left (a) The structure of biosensing based on SRR cluster (a) Microstrip transmission line top view. Right (b) Cross-sectional area of a microstrip transmission line with SRR pair and the distribution of electromagnetic field schematic [71].

changes in resonant frequency were dependent on changes in inductance and/or capacitance. As biotin and streptavidin tie to the framework the capacitance of the SRR changes which is reflected within the resonance frequency hence, it can be utilized as a biosensor.

Within the nonappearance of biomaterials, the resonant frequency of the SRR-based biosensor was 10.82 GHz. When biotin was presented, the thunderous recurrence moved to 10.70 GHz. The alter of frequency change was 120 MHz. After biotin and streptavidin were binded, the frequency moved to 10.66 GHz. The alter of frequency, in this case, was around 40 MHz. These shifts within the resonant frequency originate from the alteration within the capacitance due to the official of biotin and streptavidin [71].

Within the case of biosensors based on the resonator cluster, Lee et al. [72] also proposed a single planar twofold double split-ring resonator (DSRR) for biomolecular discovery at microwave frequencies. Compared to the SRR-based biosensor, within the absence of biomolecules, the resonant frequency of the DSRR-based biosensor was 12.35 GHz. When the ss-DNA was immobilized onto an Au surface, the recurrence was moved to 12.33 GHz. The alteration of frequency, in this case, was 20 MHz.

To distinguish cortisol, high-impedance coupled two SRRs have been realized as label-free biosensors. Estimations appeared 30 MHz and 20 MHz shifts in resonant frequency about PSA and cortisol-coupled bovine serum albumin, individually [73].

Jaruwongrungsee et al. proposed a microstrip-coupled SRR structure integrated into microfluidics as a label-free biosensor. A 6.5–13 MHz shift in the resonance frequency of the SRR was measured by S21 when IgG binding was performed on the SRR surface [74].

For glucose detection, Sathyanath et al. reported SRR- and CSRR-based microwave glucose biosensors were created, and the sensitivity was detailed as 0.174 MHz/mgml^{-1}. Also, Byford et al., 2015 reported a microfluidic multichannel resonator based on open split ring resonators (OSRR) which worked as a glucose biochemical sensor [75].

In the case of biosensors in the RF domain, Torun et al. presented a biosensor consisting of an SRR-based resonator with an integrated monopole antenna which showed a sensitivity of 3.7 MHz/(μg/ml) corresponding to changes in heparin concentration [71].

Other examples include biosensors based on a planar SRR fabricated along with a pair of microstrip antennas for the detection of glucose [76]. In this proposed biosensor design enzyme was applied to the sensor and it was tested on different glucose concentration levels. A sensitivity of 0.107 MHz/mgml^{-1} was estimated from the slope of the linear fit. Another example consists of an array resonator using the near field for pulse detection [77,78]. A hairpin resonator using a microfluidic channel based on a PDMS cover plate and SU-8 cell trapping structures for the detection of melanoma, exhibiting the S-parameters at resonance frequencies of around 2.17 GHz [79].

For the millimeter wave (mmW) range in the GHz domain, a substrate-integrated waveguide cavity resonator was presented in Ref. [80], followed by a G-shaped metamaterial absorber-based sensor for the detection of various oils [81]. A new metamaterial-based sensor utilizing the split ring resonator (SRR) along with a microstrip line was realized by Abidin et al. for the characterization of cooking oils [82]. The novelty of their work is that the mmW frequency enhanced the sensor's sensitivity for the case of liquid materials. Due to the operation in the mmW frequency range, a high shift in the transmission coefficient was observed while operating at 30 GHz [82].

Some of the recent works include the determination of change of the HSA concentration in water solutions and mixtures of enzymatic reaction due to the shift of resonance frequency by Kuznetsova et al. The work elaborated the understanding of wave reflection coefficient behavior via numerical modelling. Optimization of the metal-dielectric metasurface at microwaves was helpful for biomedical applications [83]. Another work by Bazgir et al. exhibiting the development of a high-Q factor sensor in the microwave region. This sensor was used to measure permittivity. Specific tunning was used to have operating region in the 3.36 GHz with two coupled split-ring resonators (SRRs) being the structure configuration [84].

Microwave biosensors have grown in popularity due to the numerous benefits they provide. The most essential feature is that it is non-invasive and label-free along with great sensitivity, selectivity, and real-time monitoring of biological reactions [35]. However, GHz domain-based biosensors using metamaterials and metasurfaces can face challenges most in fabrication techniques compared to the THz and optical frequency bands. Fabrication of metamaterials and metasurfaces in the GHz range can be challenging due to relatively large feature sizes. Conventional lithographic techniques used for microfabrication are typically designed for smaller nanoscale dimensions and may not be suitable for GHz-scale structures. Special fabrication methods such as e-beam lithography or direct laser writing may be required to achieve the desired pattern and resolution. Choosing suitable materials for GHz-range metamaterials and metasurfaces can be challenging. The material chosen should have low loss and exhibit desirable electromagnetic properties at GHz frequencies. To achieve the desired biosensor response and performance, it is important to consider the electrical conductivity, permittivity, and magnetic permeability of the material. Integration of metamaterial or metasurface structures with biosensor components can be complex. Biosensors often require functionalization with biomolecules or receptors to selectively capture target analytes. Ensuring proper alignment and compatibility between biosensing elements and metamaterials/metasurfaces can be a technical challenge in the fabrication process [35,52,85]. The use of biosensing in the THz range may overcome some of the manufacturing challenges in the GHz range in terms of miniaturization, advanced fabrication techniques, material selection, and spectral signatures [52].

3.2. Metamaterial and metasurface-based biosensors in the THz domain

Unique characteristics of terahertz waves set them apart from microwaves and X-rays. The non-ionizing nature of terahertz waves is one of their intriguing characteristics. This characteristic makes terahertz waves harmless to the target substance during wave-material interactions, which is a crucial characteristic for biosensing [86,87]. Terahertz waves can detect many molecular rotational and vibrational modes that are not visible to conventional mid-infrared spectroscopy [88]. Another benefit of terahertz waves is that they

easily penetrate non-polar substances and non-metallic materials (cloth, paper). This makes non-destructive detection and analysis possible. The transient electric field is also measured by coherent detection-based terahertz instrumentation. Kramers-Kronig analysis is not necessary to determine the sample's absorption coefficient and refractive index from amplitude and phase. The terahertz sensing field benefits from the characteristics [89–93].

The low spatial resolution and confinement of terahertz devices due to the diffraction limit, as well as the feeble response of terahertz waves to the majority of naturally occurring materials, pose certain challenges. As a result, by improving terahertz waves' interaction with them and their ability to be contained in space, metamaterials may be able to provide potential solutions for the implementation of reliable sensing. Terahertz metamaterial sensing has practical promise in biological and other domains since it can be tuned for amplitude, phase, impedance, and polarization [51]. The biosensing applications of metamaterial and metasurfaces based on different materials (single element, 2D elements, and hybrid) are mentioned in the following parts.

Single-Element (Noble Metals) Currently, most metamaterials with desirable properties are fabricated from common or noble metals such as gold (Au), silver (Ag), aluminum (Al), or copper (Cu) [58]. For example, Wu et al. demonstrated a self-referenced sensing method in reflection geometry for the characterization of aqueous solutions based on terahertz metamaterials. The THz metamaterial sensors used in this study are periodic arrays of gold (80 nm thick) split ring resonators (SRRs) built on a GaAs substrate [94]. In addition, it was demonstrated through numerical simulation that the frequency shift and amplitude modification were caused by the dielectric constant of aqueous solutions. This approach was helpful for the monitoring of genuine aquatic biosystems and ecological water systems.

There were very few reports on water solutions sensing based on THz metamaterials, this work was crucial for further research toward label-free, highly sensitive, real-time, and high throughput biosensing that exploits the THz-based sensing techniques for aqueous solutions.

Another example of a metamaterial-based biosensor capable of sensing a considerable shift in the resonance frequency due to the change of the dielectric environment on the metamaterial (MM) chip includes the works of Yang et al. who have developed a sensitive, label-free method for identifying transgenic plant genomes. In their work, a THz MM-based biosensor consisting of a planar array of gold (Au) split ring resonators (SRR) exhibiting a large shift in resonance frequency with changes in the dielectric environment was designed [95].

THz-TDS (time-domain spectroscopy) and finite-element simulation were used to investigate the obvious frequency shift caused by changes in the effective dielectric constant and thickness of the DNA overlayers, depicted in Fig. 3 (Left 3a-3c). Furthermore, the simulated results correspond well with the experimental data and provide a clear understanding of the sensing response to the deposited DNA film. The study reveals the THz MM biosensors' ability to identify transgenic plants in an unprecedentedly sensitive, high-throughput, label-free manner [95].

Detection of low-density viruses shown in Fig. 3 (Right 3d) [96], biomarkers such as (Aβ aggregates) [97], and label-free apoptosis measurements [98] applications were performed using gold utilizing the split ring resonator configurations. Furthermore, detection of the pesticide CM (chlorpyrifos-methyl), which is regarded as a restricted pesticide in many countries and is subject to strict maximum residue limit standards for use in agriculture was performed using CM powder, PE (Polyethylene) [99]. And, Ni was used for the label-free sensing of DNA molecules [100]. The details of the applications along with the sensor configuration and main findings are included in Table S1 of the electronic supplementary information (ESI).

In the case of metasurface-based sensing platforms, the work of Kashiwagi et al. demonstrated a simple, robust, and inexpensive method for fabricating flexible and stackable multi-resonant terahertz metamaterials using silver nanoparticle inkjet printing shown in Fig. 4 (Left 4a) [101]. Using this method, two arrays of split-ring resonators (SRRs) with different resonant frequencies were designed

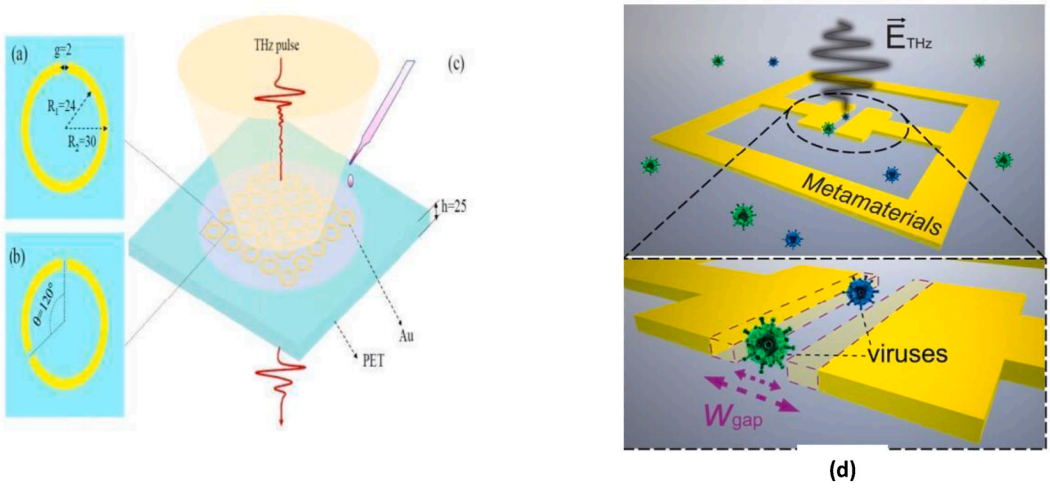

Fig. 3. Left (a) Split ring resonator (SRR) and (b) Double split ring resonator (DSRR) (metamaterial cell in a square lattice). (c) Schematic diagram of a metamaterial-based biosensor strip [95]. Right (d) Schematic of THz nano-gap based metamaterial for the sensing of viruses [96].

and fabricated on separate papers, and the two arrays were stacked and coupled; as shown in Fig. 4 (Right 4a and 4b). Another example demonstrates the introduction of paper-based MM devices that could potentially be used in biochemical sensing applications' quantitative analysis [102].

Tabatabaeian developed circular disk metasurface with a single and array of the rectangular slot based on for the detection of early skin cancer. The array of slots increased the Q-factor by more than 42.6 % along with the modification of the metasurface of 0.86 THz having a Q-factor of 1898.5. The improvement of the Q-factor was because of the use an array structure [104]. Another work of THz metasurfaces biosensor based on Fano asymmetric split ring resonators (ASRs) was proposed by Cheng et al. for the label-free detection of proteins. The work demonstrated the obtainment of 160 GHz/RIU and 240 GHz/RIU transmission dips 1 and 2 with varying refractive index of analyte from 1.3 to 1.8. The thickness of the analyte is 8 μm [105].

Various other works of metasurface-based biosensors using gold for applications in the label-free analysis of cell apoptosis, biomarker detection, and SARS-CoV-2 spike proteins detection via different split ring resonator configurations were reported [106–109]. Additionally, the detection of various microorganisms [110], determination of protein concentration [111], diagnosis and prognosis of different cancers [112], peptide identification [113], and Zika virus-envelope proteins identification [114] were also performed. The details of the configuration of metasurface and meta-structured sensors, as well as their application, the FOM, S, and LoD, are included in Table S2 of the ESI.

Single Element (2D materials) Noble metals, on the other hand, suffer from high inherent losses and non-tunability. Due to their unique electrical and optical characteristics, 2D single-element materials (such as graphene, carbon nanotubes (CNTs), and black phosphorus (BP) have recently gained substantial attention as prospective materials for sensing in the THz range. Furthermore, at high doping levels, these materials support well-confined SPPs in the terahertz frequency range [115]. THz metamaterial sensing (TMS) techniques based on 2D single-element materials exhibit high sensitivity and detection accuracy; they also exhibit good dynamic tunability via electrostatic gating and lower intrinsic losses in resonance, suggesting that they may represent a more flexible alternative to TMS methods based on conventional common and noble metals [115].

Graphene Highly sensitive sensors are made from graphene and graphene-oxides, transition metal chalcogenides (TMDCs), black phosphorous (BP), metal oxides, and other 2D materials [116,117]. SPR sensors can be designed with the help of graphene's plasmonic properties. Surface plasmon polaritons can be formed in graphene at wavelengths ranging from the mid-IR to the THz range, which is not normally seen in conventional plasmonic materials. Without altering its structural integrity, graphene is adaptable when voltage bias is applied. Unlike other 2D materials, graphene has a property that lets designers alter a structure's characteristics without altering its physical parameters. Graphene-based sensors can interact with body tissues such as the skin, eyes, brain, and muscles thanks to their thin thickness and flexible mechanical characteristics. Additionally, graphene's electrical conductivity and optical transparency enable it to produce images with high resolution making it an ideal choice for bio-tissue research. Electrophysiological data signals based on the high signal-to-noise ratio (SNR) are made possible by electrical conductivity [118–120].

High-performance ultrathin optical sensor is made possible by the combination of graphene and metamaterials [121,122]. In such sensor arrangements, a resonant wavelength arises in the reflection characteristic curve when the wave vectors of the fading waves and the surface plasmons are equivalent. Surface plasmon polaritons are produced here by electrons or photons, and they require a prism, an optical fiber, a grating, or a flaw in a metal surface [123–125]. Hence, Graphene-based biosensors or gas sensors have promising applications in the THz frequency range.

Ruan et al. developed a super-sensitive terahertz biosensor with hybrid Fano structure resonance of graphene and waveguide, as shown in Fig. 4. Plasmon excitation of graphene holds promise for the development of functional devices in the terahertz frequency band. This sensor has been demonstrated by combining the graphene surface plasmon and plane waveguide polarization modes, and the obtained Fano resonance to prepare an ultrasensitive sensor [103]. The influence of the coupling layer and the thickness of the air layer in the sandwich structure on Fano resonance is also discussed in detail and a sensitivity of 3260 RIU^{-1} is achieved. Meanwhile, Zhang et al. [126] proposed a navigable graphene terahertz sensor with dual Fano resonance and achieved supersensitive detection

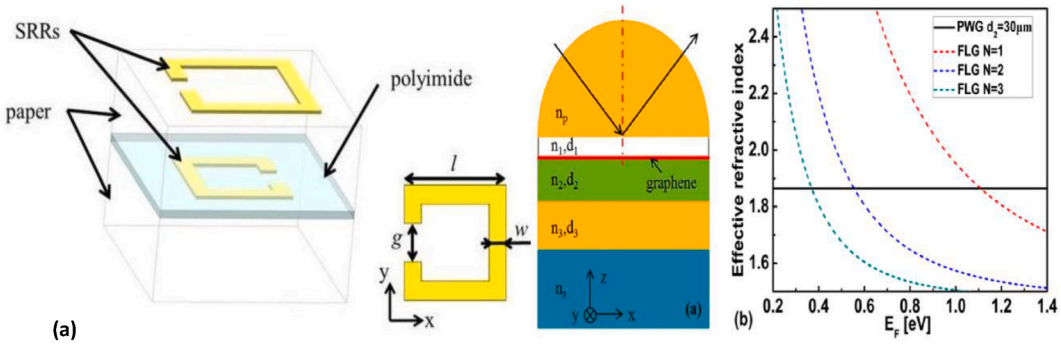

Fig. 4. Left (a) A simulation model of the split ring resonators created using the finite element method (FEM) is shown in schematic form. The length (l), width (w), gap (g), and separation between adjacent SRRs within each array serve as the primary design parameters for each of the two different types of SRRs that were utilized [101]. Right (a) Schematic representation of the Fano resonance-based biosensor suggested; (b) Effective refractive indices of graphene surface plasmon polariton (SPP) and planar waveguide (PWG) modes [103].

with 1.9082 THz per refractive index unit (RIU) and quality factor. (FOM) is 6.5662. Tang et al. [127] proposed a highly sensitive optical biochemistry sensor at terahertz frequencies, in which the detection medium is sandwiched between a composite structure containing a one-dimensional photonic crystal and graphene, consisting of polymethyl pentene (TPX)/SiO_2 as the substrate, with a layer of graphene film inserted between vertical structures,

A multi-channel structural sensor with an approximate 10 pM limit of detection was created for DNA analysis. This sensor has traits like genetic variations, disease biomarkers, and high throughput drug candidate screening [128]. Wendao Xu et al. developed a hybrid gold/graphene-based metamaterial biosensor that has ultrahigh sensitivity and can detect minute amounts of chlorpyrifos-methyl [129].

Graphene-based metamaterial sensor configurations such as different split ring resonators were used for applications in biomedical, refractive-index sensing, and environmental monitoring [130–133]. The disc-shaped graphene structures were used in the applications of gas and liquid detection [134], multi-substance detection [135], and excitation of surface plasmons [136]. The details of these graphene-based metamaterial sensor configurations, as well as their use, sensitivity, and FOM are included in Table S3 of the ESI.

Due to its low losses and highly confined surface waves, graphene is a widely preferred advanced plasmonic material for THz sensing. Graphene's structural parameters can be altered to change its tunability, which can be used to create tunable devices. Due to its hexagonal honeycomb lattice and 2D carbon structure, graphene has exceptional optical and electrical properties. Furthermore, the chemical potential of graphene can be altered by varying the gate voltage supplied to the structure. As a result, graphene is frequently used in the fabrication of tunable metamaterial sensors and is the most promising surface plasmon and tunable material in the THz band [137].

Carbon Nanotube (CNT) and Black Phosphorous (BP) Single-walled CNTs extracted from graphene sheets possess good tunability properties along with excellent chemical and environmental stability [138]. These CNTs also possess special electronic properties and large mean-free paths making them suitable for detecting in the THz region [139]. An example is the work of Wang et al. who performed THz detection of chlorpyrifos-methyl using CNT-based metamaterials [140]. The detection sensitivity obtained was better than 0.1 mg L^{-1}, which was lower than the World Health Organization interim guideline limits established for chlorpyrifos-methyl content in vegetables.

In recent years, BP has also become an integral part of the 2D family of materials, due to its wide navigable electron band gap and high electron mobility [119]. The use of BP in THz sensing applications is still in a preliminary stage and most of the published work on this topic mainly deals with theoretical simulations [141]. Liu and Aydin theoretically investigated local SPRs generated in a nanostructured BP monolayer [142]. Fo et al. further improved the signal response of the nanostructured BP monolayer in the THz frequency range and examined the local SPRs generated in the BP nanostrip array [143]. The plasmon resonance studied in this work depends heavily on the geometrical parameters of the nanostrips and the coupling between adjacent nanostructures, suggesting that these BP monolayers are prominent candidates for sensing applications in the THz region. The intrinsic losses of these materials are low compared to the common and noble metals. However, the sensing mechanism of molecules adsorbed on them must be studied in more detail [51].

Single Element (Dielectrics) Terahertz detection techniques using perfect metamaterial absorbers (MPA) based on metallic metamaterials have been extensively studied in recent years [144]. However, metal MPAs have some disadvantages, such as relatively narrow bandwidth and high resistance loss in the material [145]. Wang and associates. reported two silicon-based plasmonic metamaterial absorbers with absorption rates of 99.7 % and 99.9 %, which can be used as THz metamaterial sensors for chlorpyrifos detection [146]. Clear changes in absorption spectra were observed after the deposition of chlorpyrifos using a silicon-based plasmonic metamaterial absorber. In addition, the optical tunability of these two types of absorbers was proposed and investigated through simulation, which highlights a new strategy to control dielectric metamaterials and demonstrates a potential solution to achieve device reconfiguration for future applications. The intrinsic absorption losses observed in common and noble metals can be easily overcome by Silicon. Furthermore, silicon can also be integrated easily with the existing CMOS technology due to its tunable conductivity [51].

Hybrid Metamaterials To date, the sensitivity of label-free THz detection for traces of target substances and molecular vibrations has remained relatively low. Therefore, the generation of resonance-enhanced electromagnetic fields exhibited in hybrid metamaterials can be a potential solution to this problem [147,148]. Hybrid metamaterials possess the advantages of some magnetic materials developed artificially, which could play a key role in the THz region sensing process [116,149]. For example, a hybrid metamaterial containing Au and graphene components combines the high sensitivity and tunability of Au and graphene, respectively [145,147,150]. Zeng et al. developed a new graphene/gold hybrid metasurface configuration that has application areas in biomedical research (including early disease detection and diagnosis) [145]. This configuration exhibits increased sensitivity and allows the detection of traces of single-stranded DNA molecules at a very low concentration of 1×10^{-18} M. Another example includes the work of Xu et al. who designed a simple biosensor platform by adding a graphene monolayer on the surface of the absorption cavity of the terahertz metamaterial to make it more sensitive [151].

By optimizing the configuration of hybrid metamaterials, their sensitivity, and tunability in the terahertz range have been significantly increased. However, the utilization of hybrid metamaterials in sensing technology is still new, and additional work must be conducted to better illustrate the hybrid effects theoretically and experimentally. The identification of targets with multi-resonance peaks can improve the detection accuracy and these hybrid materials characterized by this phenomenon can attract potential applications in the biosensing field [51].

Metamaterials and metasurface-based biosensing in the THz range have not been fully or partially commercialized due to some potential reasons THz-based sensors via metamaterials and metasurface using common noble metals (Au, Ag, Al, Cu) are expensive due to the cost of lithography. In the case of 2D single-element materials (graphene, carbon nanotubes, and boron phosphorous), the materials themselves are very expensive. In addition, the materials are non-reusable which in turn increases the price of the sensors.

The THz-based sensors from dielectric such as silicon, the sensitivity is low [51]. Based on these points, the characteristics of the materials for sensing applications are summarized in Table S4 of the ESI.

Terahertz (THz) Microfluid-based Biosensing in Metamaterials and Metasurfaces The limitation of THz-based sensors is the strong absorption of THz waves by water restricting the specimen category to dry or partially hydrated. Reduction of the liquid amount in the specimen is important for THz biosensor application expansion. The use of microfluid chips can overcome the THz wave absorption. The advantages of microfluid chips are low cost, fast analysis, and less sample volume requirement [151].

THz sensor based on a toroidal dipole resonance metasurface with a microfluid channel integration was proposed by Chen et al. The calculated Q-factor and FOM reached 1103 and 244 respectively. The refractive index sensing of non-polar and polar liquids upon investigation showed that the shift in resonance frequency does not rely on analyte losses [152].

Zhou et al. proposed a THz-graphene metasurface microfluid platform by the incorporation of graphene with a THz metasurface into a microfluid cell [153]. For sensing mechanism verification, experiments on pure microfluid cells, metasurface-based cells, and graphene-based microfluid cells were conducted. The high sensitivity was observed in the hybrid-graphene metasurface THz microfluid device [151].

One illustration is a label-free biosensor that was combined with microfluidics and was based on a split ring resonator (SRR). The proposed sensor was implemented for immunoglobulin G (IgG) detection [154]. On RT/duroid 60102, the SRR configuration was put into practice. PDMS (formed using the mold-casting technique) was used for the LM and the microfluidic channels. When the concentration of IgG is increased from 50 to 200 μg/mL, the resonance frequency of the split ring resonator (SRR) shifts by around 6.5–13 MHz (measured by S21). A novel multi-microfluidic-channel metamaterial biosensor (MMCMMB) based on bow-tie array metamaterial with multi-channels consisting of equilateral triangles was proposed by Zhang et al. for the sensing of small-volume liquid sensing [155]. The proposed design (bow-tie array metamaterial with multi-channels) was highly sensitive, compatible, label-free, cost-effective, and easy to operate. The sensing results based on isopropyl alcohol (IPA)-water mixtures and bovine serum albumin (BSA) solutions demonstrated the effectiveness of the proposed sensor configuration and its potential in THz bio-sensing.

Terahertz biosensors based on one gap split ring resonator and two gaps split ring resonator have been proposed for the early detection of the liver cancer biomarkers AFP and Glutamine Transferase Isozymes II (GGT-II) [156]. Water could not be absorbed into the target biomolecules because of this design. This obstacle typically emerges at terahertz frequencies. Resonance shifts of approximately 19 GHz (5 mu/mL) and 14.2 GHz (0.02524 μg/mL) were observed for GGT-II and AFP with a two-gap metamaterial, respectively. The two types of SRRs in this work have been designed, fabricated, characterized on bulk silicon substrates, and integrated into microfluidics for biosensing applications. Test results for two liver cancer biomarkers, AFP, and GGT-II, showed agreement between experiments and simulations.

Hence, liquid-based biosensing in the THz region can be possible via the integration of a metasurface and microfluid-based platform advancing the development of THz microfluid-based labs-on-a-chip.

3.3. Metamaterial and metasurface-based biosensors in the optical frequency domain

The optical spectrum is commonly characterized as electromagnetic radiation with wavelengths ranging from 10 nm to 10^3 μm, or frequencies ranging from 300 GHz to 3000 THz [157,158]. These biosensors enable detecting and studying binding events between the target analyte and its corresponding receptor on metal surfaces [35]. The plasmonic biosensor is based on surface plasmon resonance using surface plasmon polarization (SPP). Due to the resonant photon-SPP coupling conditions, surface plasmon polarizers can provide very small detection limits over 10^{-5} refractive index units (RIUs) [35].

SPR-based systems require optocouplers (prisms and gratings) with a narrow operating range and short detection distance performance. As a result, it becomes difficult to integrate with low-cost, high-throughput, and real-time biochips for rapid bioanalytical measurement of limited-quantity samples. Therefore, surface polarized plasmon (SPP)-based biosensors improve the sensitivity for detection of small analytes towards nanoscale design and adjust biochemically selective nano configurations based on size at the nanometer scale [35].

The localized surface plasmons of metal nanostructures lead to a strong enhancement of the local electric field and spectral tunability [159–161].1 However, the detection performance of the sensor is based on local surface plasmon resonance (LSPR) based on the change in the refractive index with a sensitivity not exceeding 100–300 nm/RIU in the spectral interrogation sample [35]. Plasmonic metasurfaces (bowties, nanopillars, nanoholes, apertures/cravings) are widely used to enhance interactions in biosensing between light and biomolecules by the effect of near-field confinement [162].

Monteiro et al. used a gold nanohole array with transmitted light intensity for monitoring TNF-α which is an inflammation-related protein assay for disease diagnosis that achieves a sensitivity of 4000–5300 IU/RIU and an LOD of 17 pg/mL [163]. Khan et al. provided an idea for using DNA aptamers to monitor other biological interactions. With strong versatility, resistance to denaturation, and substrate retrieval advantages [76], DNA aptamer-functionalized gold nanodisc arrays achieved a bulk sensitivity of 113 nm/RIU based on LSPR absorbance spectroscopy, with a limit of detection (LoD) of 1 0.49 ng/mL with a dynamic range of 1.7–20.4 ng/mL for low PSA detection [164]. As advances in nanofabrication and materials design continue, plasmonic metasurfaces will play an increasingly important role in the development of the next generation of plasmonic sensors (biosensors) with improved sensitivity, precision, and multiplexing capabilities is expected. Furthermore, optical metasurfaces containing nanoscale building blocks that support strong mode coupling have attracted considerable interest among researchers in recent years [165–168]. Essentially, the Fano resonance is the continuous (bright mode) and discrete non-radiative (dark) modes of scattered waves [169].

In addition, we can further divide the optical frequency range into near mid-infrared and optical regime. Therefore, a special structure i.e., nano-antennas have arisen as a hot topic in recent decades because of their good performance and energy augmentation

when the electromagnetic wave or light is incident to these structures in the visible or infrared domains [170]. In summary, these configuration of these nanoantennas can be of nano aperture and nanoelement. Sensing platforms based on the aperture configuration can be used for the biosensing applications [171]. A dual-resonant nano-antenna array based on the aperture configuration of complex rectangular fractal was introduced by Aslan et al. for ultra-sensitive biosensing and chemical applications [172]. Another example includes the works of Cetin et. all where numerical and experimental results were demonstrated based on the dual-resonant metamaterial based on subwavelength Jerusalem cross-shaped apertures, a good candidate for optical applications [173].

Another multi-resonant metamaterial structure based on the integration of U- and T-shaped nano-aperture antennas for the use of biosensing was exhibited by Turkmen et al. for infrared detection applications[174]. It was established how the suggested structure's spectrum response will behave for various geometrical parameters and substrate types. The observance of the regularity brought about by the varieties of membrane materials, membrane thickness, thickness of the metal layer, and aperture width was demonstrated [174]. In order to develop a novel arrangement of the nanoantenna for Fano resonance a U–I array structure for mid-infrared applications was proposed by Zarrabi et al. The FOM factor was analyzed and compared for each resonance with the purpose of assisting biosensing applications. The results indicated that the Fano resonance exhibited the highest value of the FOM factor when compared to the plasmonic mode at U-array structures making the Fano resonances useful for more precisely separating materials in the optical regime [175].

Among the recent works, based on a checkerboard pattern configuration, a novel metasurface has been developed for optical biosensing in the infrared region for the identification of cancer cells at an early stage. Compared to traditional metasurfaces with a single resonance, the suggested metasurface enables the identification of unknown materials with a better degree of precision. At 47.4 RIU−1, the maximum FOM is accomplished, and the maximum Q-factor attained is roughly 354. Furthermore, the sensitivity factor increases to a maximum value of 3657 nm/RIU, which improves the metasurface's sensing capacities even more [176].

Optical metasurfaces, which are nanopatterned surfaces with two dimensions and the ability to control light, have great potential for accurate virus identification. Examples include the design of a fractal plasmonic metasurface-based for an extremely sensitive biosensor in the near-infrared light range [177], using of a dielectric metasurface for optical trapping on the enhancement factor in Raman spectroscopy [178] for virus detection. In terms of bacteria detection, a pentamer and split ring resonator (SRR) hybrid structure formed the basis for a suggested and simulated dual band plasmonic absorber. A sensitivity around 450 nm/RIU and a Figure of Merit of 227 RIU^{-1} was observed for the optimized structure [179]. Another cutting-edge multi-layer absorber based on the metal-DNA-metal structure demonstrated that a redshift may be obtained by switching the organic portion to "High Configuration" mode. For designing an optical sensor with switching behavior, DNA composite is being studied. The FOM of 735 RIU−1 was recorded, surpassing the FOM of conventional absorbers for the purpose of refractive index sensing [180].

Some other examples include the metal-insulator-metal and all dielectric metasurface for the biosensing applications. Furthermore, multimode plasmonic sensors are very beneficial since they may perform better than their single-mode equivalents because of multimode data cross-referencing, improved information retrieval, and long-wavelength tuning. Khan et al. proposed silver square block arrays (SSBs) in a metal−dielectric−metal arrangement to concurrently obtain a high-quality factor and increased sensitivity depicted in Fig. 5 (Left 5-a). When combined, the suggested sensor shows promise as a first screening tool for different kinds of biomolecules and can recognize a wide range of biomolecules [181]. Another suggested and studied nanostructure is based on the combination of graphene, plasmonic, and black phosphorus shown in Fig. 5 (Right 5-b). The modified structure would be used as refractive index sensors to measure blood samples' amounts of hemoglobin, creatinine, and cholesterol. Significant sensitivity factors for the concentrations of cholesterol, creatinine, and hemoglobin are found to be 5333.3 nm/RIU, 1562.5 nm/RIU, and 800 nm/RIU, respectively [182].

In terms of all dielectric metasurface, A tunable design of silicon resonators based on an all-dielectric metasurface design that consists of a nanodisk and a nanobar, two polycrystalline silicon resonators, was published by Salama et al. depicted in Fig. 6 (Top 6a and 6b). At the working wavelength of ($\lambda = 1.583\ \mu$m), the structure's sensitivity was (275nm/RIU), resulting in a figure-of-merit (FOM) of (148). Because of its excellent performance and simplicity of manufacture, the suggested design shows great promise for use in refractometric biosensing applications [183]. In addition, Chen et al. presented an all-dielectric metastructure shown in Fig. 6

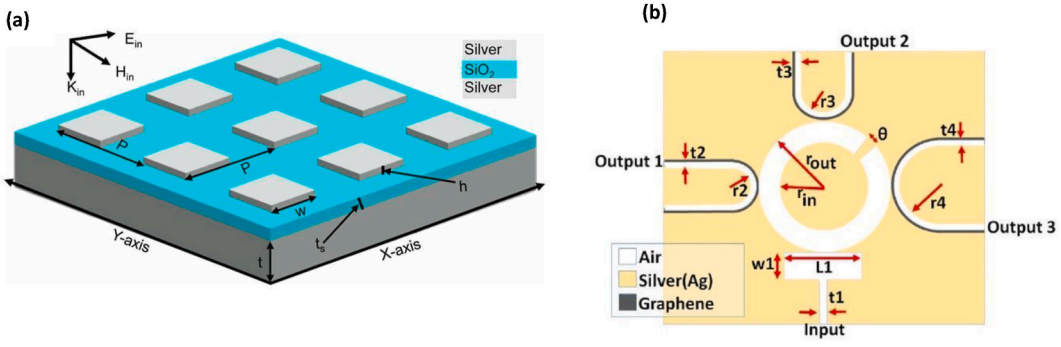

Fig. 5. Left (a) Schematic diagram of the proposed metal-insulator-metal (MIM) metasurface in the infrared region [181]. Right (b) Schematic diagram of the proposed plasmonic-graphene structure [182].

(Bottom 6a and 6b) that consists of a crossing rod and four fan-shaped silicon blocks that are periodically put on a silicon dioxide (SiO2) substrate. The suggested metastructure has outstanding sensing qualities, as demonstrated by the simulation findings, which include a Q-factor of 3668, sensitivity of 350 nm/RIU, and figure of merit (FOM) of 1000. There are potential uses for the metastructure in the field of refractive index sensors [184].

Fano-resonant Based Metamaterials and Metasurfaces in Biosensing In the context of plasmonic nanostructures, the coupling between the broad-band super-radiation mode and the narrowband sub-radiant mode produces the Fano-resonance. Extinction interference develops because of the frequency overlap between these two resonant modes [185–187]. This phenomenon suppresses the system scattering by a narrow band. As a result, the steep scattering cross-section causes an asymmetric Fano spectrum line shape to emerge in the scattering cross-spectrum along with high sensitivity [188]. The equations of Fano resonance in terms of simple coupled oscillators is included in Equations 1 and 2 in the ESI [31].

The optical response of any resonant system has a Lorentzian shape [189]. This phenomenon is real for plasmonic nanostructures when just one resonance, like a tiny particle or dipole antenna, is excited. The line shape, which has various peaks, becomes extremely complicated when there are multiple resonances. The Fano-line shape is significant among such erratic reactions.

This brand-new kind of resonance with an asymmetrical spectral line shape was found in 1961 by Ugo Fano [190]. According to the field of nanoplasmonics, Fano resonances can happen when two modes—bright and dark—are present in the system. While the dark mode does not radiate into the far field (like a quadrupole), the bright mode does (as in the case of a dipole) [185].

The structures' radiation loss is decreased by fano resonance. Sharp, asymmetric line shapes and quick phase- and amplitude changes are two important features of Fano resonance. Such properties have their roots in coherent coupling and interference between discrete and continuum states. Split ring arrays, hole/particle arrays, plasmonic nanocavities, and diffraction gratings are just a few examples of plasmonic nanostructures and metamaterials that exhibit fano resonance. Sensing, optical transmission, electro-optical modulation, and switching are some of the uses for Fano resonance [118]. Fano resonances can be used in systems like photonic crystal plasmonic structures [166,185,190–192] and metamaterials [193–196]. The sensing capabilities of the plasmonic

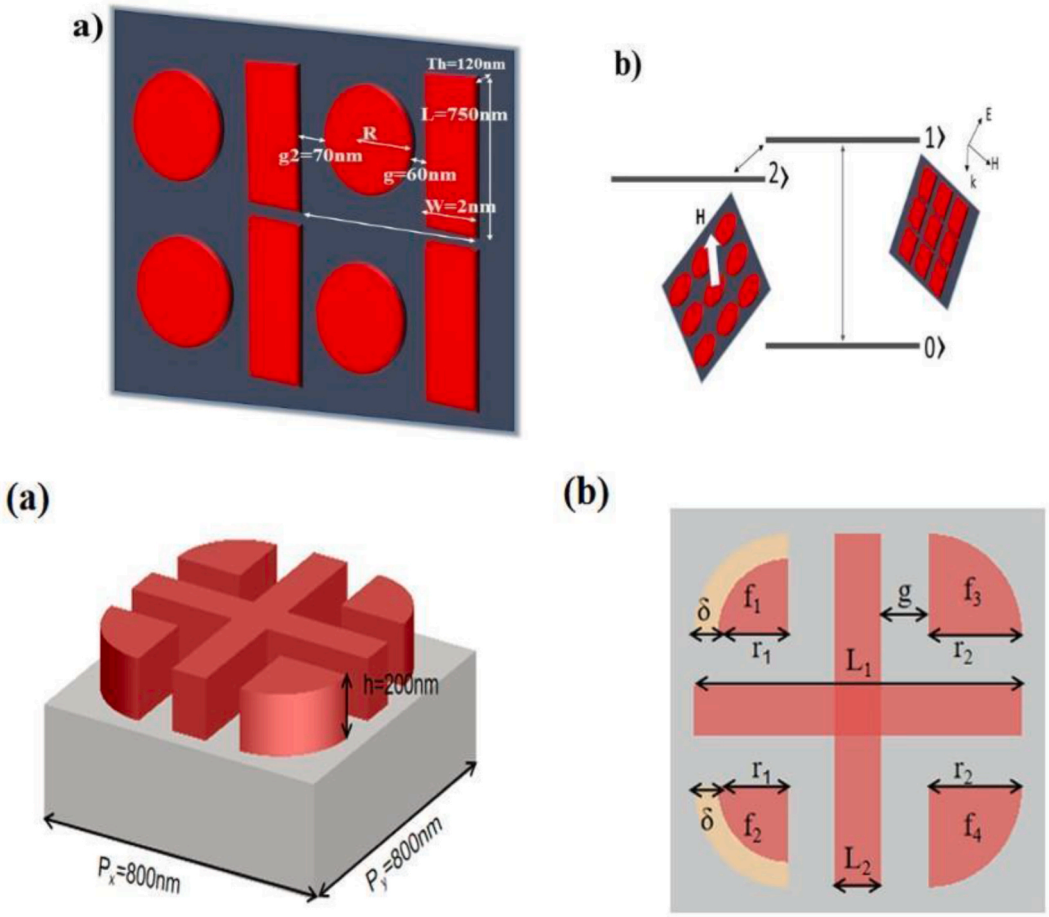

Fig. 6. Top (a–b) Schematic diagram of the Fano resonant based all dielectric metasurface design [183]. Bottom (a–b) Schematic representation of a single cycle of the intended meta-structure, which consists of four silicon blocks shaped like sectors and a cross rod positioned on a silica substrate [184] (For interpretation of the references to colour in this figure legend, the reader is referred to the Web version of this article.)

metamaterials can be enhanced by characteristics brought on by adjusting the line shape of the Fano resonance, which can result in small FWHM and strong field enhancement [197].

Examples include electromagnetically induced transparency (EIT), such as Fano resonances, which have a small linewidth of about 153 nm. It was observed in complementary planar metamaterial H-shaped cutout nanostructures. A metamaterial sensor based on this Fano resonance demonstrated a high sensitivity of 588 nm/RIU and an FOM of 3.8 [198].

Fano resonances with significantly enhanced electromagnetic fields were seen in the cavity under the introduction of material layers in the asymmetric ring/disc nanocavity array. This cavity system, with a full width at half maximum (FWHM) as small as 9 nm, supports fano resonance. The RI sensitivity of the Fano resonance-based metamaterial sensor is 648 RIU/nm, and the FOM is 72. This Fano-resonant metamaterial sensor is used to detect mono- or bilayer proteins with high sensitivity as depicted in Fig. 7 (Top 7a and Bottom 7b) [199].

Another illustration involves the realization of a plasmonic nanohole array using strongly dispersive plasmonic Fano resonances and related wood anomalies, which allowed for the direct visual detection of an antibody monolayer. Because of the interference between light traveling through the holes and scattered surface plasmon polariton (SPP) modes enabled by the hole arrays, these plasmonic nanohole arrays display Fano resonances. With a FOM of 162, the experimental RI sensitivity was approximately 717 nm/RIU [200].

To detect Fano resonance-based high-performance sensing, an array of sub-micrometer gold mushrooms, each consisting of a gold (Au) cup on top of a photoresist pillar positioned within a hole in a gold film, was also used. Due to Fano resonance, the RI sensitivity and FOM were both up to 108, with an RI sensitivity of roughly 1015 nm/RIU. This sensor's limit of detection (LoD) for cytochrome C and alpha-fetoprotein (AFP) was around 200 pM and 15 ng/mL, respectively [201].

Hyperbolic Dispersion-Based Metamaterials and Metasurfaces in Biosensing Label-free detection and quantification of nanosized objects in biosensing applications is a challenge because of the deficit of highly sensitive, cost-effective, and reproducible techniques. The sensitivities of existing plasmonic sensors are not that high enough for the detection of low molecular weights or the low surface

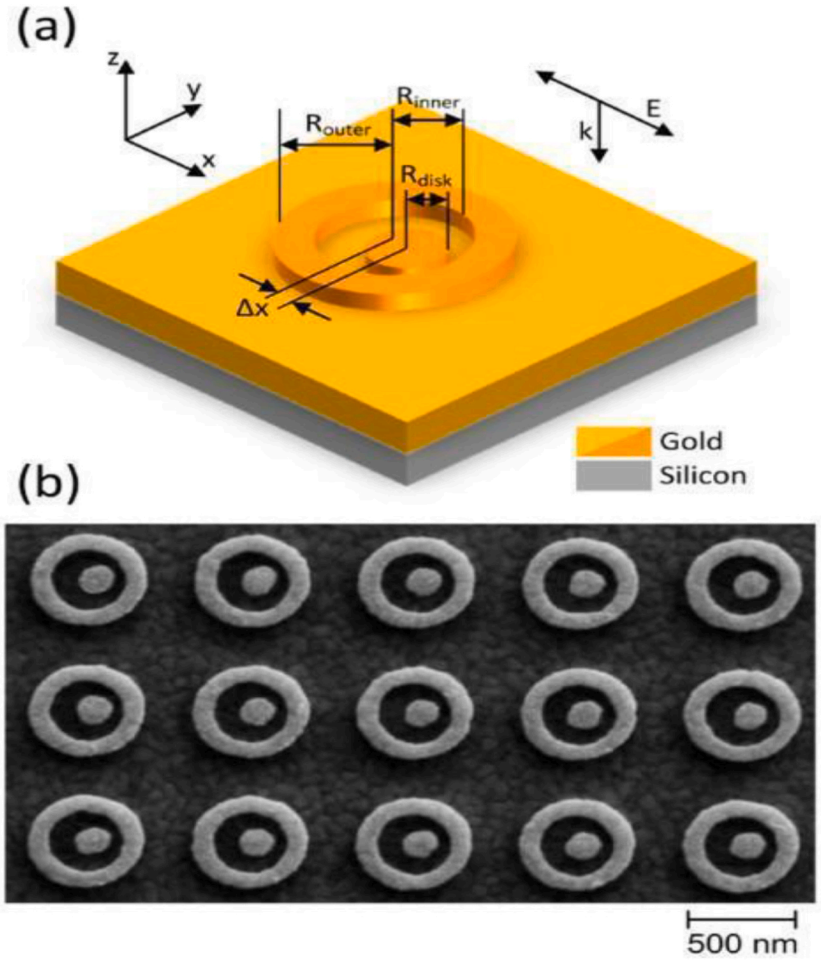

Fig. 7. Top (a) A schematic representation of a fabricated asymmetric ring/disc system; Bottom (b) A scanning electron microscope (SEM) image of the fabricated asymmetric ring/disc cavity [199].

coverage of exceedingly small molecules [202].

Optically active metamaterials with anisotropic permittivity, called hyperbolic metamaterials (HMM) have large-scale 3D sub-wavelength structures. HMMs are a subclass of artificial anisotropic materials that exhibit hyperbolic dispersion [57]. Since the out-of-plane dielectric component $\varepsilon_{zz} = \varepsilon\perp$ and the in-plane dielectric components $\varepsilon_{xx} = \varepsilon_{yy} = \varepsilon||$. have the opposite signs, dispersion results. The hyperbolic dispersion relation of HMM (uniaxial anisotropic material) is $(k_x^2 + k_y^2)/\varepsilon_{zz} + (k_z^2)/\varepsilon_{xx} = \omega^2/c^2$, where tensor $\varepsilon = [\varepsilon_{xx}, \varepsilon_{yy}, \varepsilon_{zz}]$ gives the dielectric response [202]. Metal nanorods in a dielectric host (Type I) and ultrathin metal-dielectric multilayers (Type II) are the two types of HMMs [184]. The equations of hyperbolic metamaterials based on effective medium theory is included in Equations 3 and 4 in the ESI [31,203].

In the effective medium limit, these materials support waves with infinitely large momentum called bulk plasmon polariton (BPP) because of the hyperbolic dispersion. These bulk plasmon BPPs can spread within the HMM. However, in the substrate, these waves vanish and exponentially decay. While type II HMMs only support high-k BPP modes, type I HMMs support both high-k and low-k modes [184]. HMMs have a wide range of possible applications due to their capability for high wave-vector (k) propagating modes. The uses include nanoimaging, spontaneous enhancement, perfect absorption, and negative refraction. in addition to the creation of plasmonic biosensors with extreme sensitivity [204].

The extinction and reflection spectra of hyperbolic nanorod metamaterials depend on the plasmonic response of each nanorod inside the assembly and the electromagnetic coupling between them. Because of the oblique illumination, these metamaterials are necessary for sensing applications [205].

Label-free biochemical sensing with extraordinarily high sensitivity can be achieved using plasmonic hyperbolic metamaterials based on nanohole arrays. A gold (Au) nanorod metamaterial attached to a prism's surface and illuminated further using attenuated total reflectance (ATR) geometry makes up a typical sensing setup. This nanorod metamaterial's refractive index sensitivity and FOM were 32,000 nm/RIU and 330, respectively. Furthermore, it was predicted that the biotin detection limit of this metamaterial-based sensor would be lower than 300 nM [206].

The creation of high uniformity nanorod hyperbolic metamaterials helped to further improve the method. Electrodeposition and electron beam lithography (EBL) were both used in the fabrication process. The sensor had a high FOM of 416 and an RI sensitivity of 41,600 nm/RIU. Due to the EBL fabrication method and resonance narrowing, the nanorods in the array were arranged more regularly, which improved sensing performance [207].

Along with nanorods, co-axial rod-in-tube metamaterials and nanotubes have been developed and employed for optical sensing [208,209]. Nanorod metamaterials need to be illuminated with TM-polarized light in an oblique or ATR-based manner. Their refractive index (RI) sensitivity is less than 300 nm/RIU lower than that of the waveguide mode in nanorod metamaterials.

Miniature grating-coupled sensors based on layered hyperbolic metamaterials were developed to replace bulk-size prism-based ATR setups [197]. One of the suggested metamaterial sensors is an Au/Al_2O_3 multilayer hyperbolic metamaterial. The sensor configuration also includes a microfluidic flow channel and a 2D metallic nanohole diffraction grating. A wide range of wavelengths can be supported by the proposed hyperbolic metamaterial's confined bulk plasmon-guided mode. With a sensitivity of 30,000 nm/RIU and a FOM of 590, the sensor was used for the picomolar detection of ultralow molecular weight (244 Da) biomolecules [210]. By combining metamaterials and optical fibers, HMM-based biochemical sensors can be made smaller (D-shaped fibers) [197].

Multiple periodic Ag and TiO_2 bilayers with a 30 nm thick are present in hyperbolic metamaterials. In contrast, few-mode fiber has a residual fiber thickness (RFT) of 72 μm. The FOM is 230.8 RIU^{-1}, with 9000 nm/RIU being the highest sensitivity in the nearby refractive index (1.33–1.40 RIU) [211].

Another example is an SPR optical fiber design that incorporates a 3D Au/Al_2O_3 composite HMM, a graphene sheet, and a D-shaped plastic optical fiber (D-POF). The suggested G/HMM/D-POF sensor has a high sensitivity (4461 nm/RIU) as well as strong linearity, stability, and reproducibility. One application for the biosensor is the measurement of concentration- and time-dependent DNA hybridization kinetics [212].

Creating a brand-new HMM/D-POF SPR sensor involved synthesizing and fabricating Ag/MgF_2 layered hyperbolic metamaterial. The sensor exhibited high sensitivity, k-transfer mode, and multimode coupling oscillation. The sensor, which was used to detect saccharin and BHT (representatives of substances linked to cancer), had a sensitivity of 1875 nm/RIU [213].

A colloidal form of hyperbolic materials known as meta-particles also achieves high refractive-index sensitivity. It is easier to fine-tune the interaction of plasmonic nano-objects with light when they are coated with an anisotropic metamaterial with hyperbolic dispersion. As a result, dielectric nano-objects with hyperbolic coatings, where the nature of modes is related to the hyperbolic layer resonances. These metaparticles have a refractive index sensitivity of 740 nm/RIU and could be useful in high-resolution optical sensing [214]. Furthermore, a hybrid platform made of graphene and Sb_2S_3–TiN HMM in apta-biosensor platform configuration was used for the determination and binding of thrombin concentration in real-time with a Limit of detection (LoD) 1×10^{-15} m [215].

Biosensing at the Interface between Chiral Metasurfaces and Hyperbolic Metamaterials The interface between hyperbolic metamaterials and chiral metasurface can enable both high sensitivity and specificity for the detection of low molecular weight [202]. When an object's mirror image cannot be overlaid on it using any combination of translational or rotational operations, it is said to be chiral [197]. So chiral metamaterial is a special kind of material where molecular interactions are seen. Nature is filled with instances of chirality, including the left, right, and circular polarizations of light as well as the spin of elementary particles, chemical molecule configurations, and elementary particle spin [197]. Additionally, optical materials exhibit chirality. These materials' chirality allows for the display of various optical characteristics for light that is circularly polarized but has a different handedness. Optical birefringence and circular dichroism (CD) are the two effects that result from it. Right circularly polarized (RCP) and left circularly polarized (LCP) light pass through a medium with different propagation constants, which are associated with different real parts of their refractive indices. This is referred to as optical birefringence. In contrast, circular dichroism (CD) is linked to numerous fictional

components of their refractive indices. In this case, the LCP and RCP light states are absorbed differently. The combined effects of optical birefringence and circular dichroism determine the medium's optical activity [197].

The material's chirality also suggests a coupling between its magnetic and electric responses. The magnetic response at optical frequencies is not strong for natural materials. As a result, the chiral optical properties are also minimal. To achieve the necessary optical activity effect, light must therefore travel over macroscopic distances in the medium. With resonant effects, particularly, metamaterials can enhance the media's optical and magnetic response. Metamaterials can also offer a platform for optical materials to have improved chiral properties (chiral metamaterials). A collection of spiral-shaped metallic nanowires would serve as an illustration of chiral metamaterial design [197].

Both naturally occurring chiral biomolecules and man-made chiral molecules have different chemical and physical properties depending on their chirality [216,217]. A strong optical field can be produced in the near field by chiral metamaterials, which offers a desirable platform for biomolecule chiral sensing [59].

The optical excitation of plasmonic planar chiral metamaterials generates superchiral electromagnetic fields, which are extremely sensitive indicators of supermolecular structural chirality [218]. In this study, left- and right-handed plasmonic chiral metamaterials (gold gammadion arrays) were created on a glass substrate for use as planar chiral metamaterials. Their circular dichroism (CD) spectra were nearly identical.

Furthermore, employing left- and right-handed twisted optical metamaterials, ultrasensitive (zeptomole scale) detection of chiral compounds was achieved depicted in Fig. 8(a–d) below [219].

According to the literature, the measured molecule concentration in the imaging area was as low as around 55 zmol, or 44 molecules per unit cell of the metamaterial, which is 10^{15} times less than the detection capabilities of conventional commercial CD spectroscopy equipment [219].

Additional research has demonstrated the ability of Shuriken metamaterials (chiral plasmonic metamaterials) to discern tertiary/

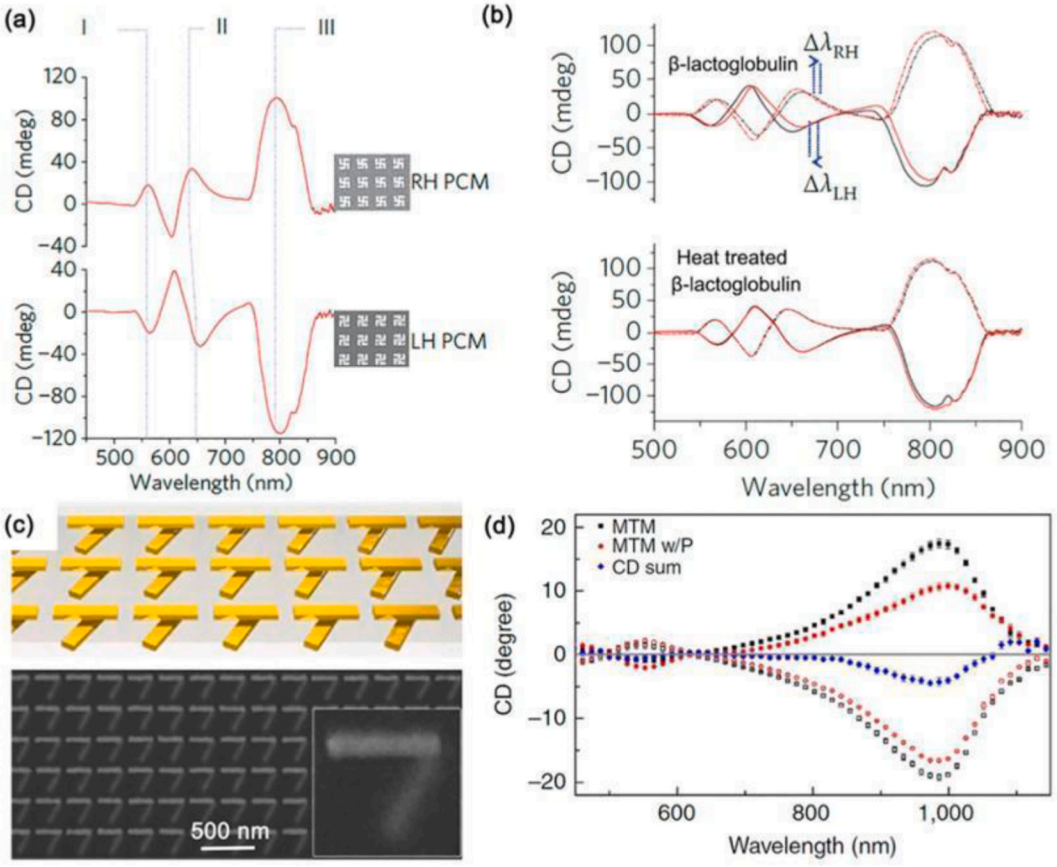

Fig. 8. (a) Distilled water-submerged left- and right-handed gold gammadion arrays, as well as circular dichroism spectra and SEM pictures of the matching chiral metamaterials (in the inserts). (b) The effects of thermally denatured absorbed proteins -lactoglobulin and -lactoglobulin on the CD spectra of chiral metamaterials. (The solid line represents left-handed chiral metamaterial; the dashed line represents right-handed metamaterial.) (c) A +60° twisted metamaterial SEM picture and schematic. (The red spectra were collected before protein adsorption in Tris solution, while the black spectra were collected after protein adsorption.) The CD spectra of the metamaterial in panel c functionalized with a monolayer of protein (Concanavalin A) for ±60° twisted metamaterials are shown in (d); (solid symbols signify +60° metamaterials, and empty symbols denote −60° metamaterials) [219] (For interpretation of the references to colour in this figure legend, the reader is referred to the Web version of this article.)

quaternary (higher-order) proteins' hierarchical structures at the pictogram level [220]. Furthermore, the structural order of proteins in complex bio-interfaces was investigated, as well as the sensing of proteins with identical structures but distinct primary sequences by a single amino acid [221,222].

Modified out-of-plane chiral metasurfaces can enable three functionalities of the hyperbolic metamaterial-based sensor. One is the efficient diffractive element for SPP and BPP excitation. The second is the increase of the total sensing surface forced by out-of-plane binding. Amplification of chiral-chiral interactions between the metamaterial incorporation and molecules via optimal tuning of circular dichroism (CD) and chiral selectivity enabling high-sensitivity detection of enantiomers [222].

An example includes a chiral metasurface hyper-grating (CMH) consisting of a periodic array of right-handed gold (Au) helics on a type-II HMM composed of indium tin oxide (ITO-20nm) and silver (Ag-20 nm). The configuration from top to bottom consists of a superstate containing the Au helics multilayer system (gray stack ITO/Ag) and glass substrate. Reflectance minima (mode dips) of the coupled systems were calculated and exhibited redshift with the increase of the refractive index from water (1.333) to 1.401 (around 17 % molar fraction of $C_3H_8O_3$). The limit of detection (LoD) is equal to 1.5×10^{-4} RIU [223,224].

4. Challenges and future outlook

Sensitive biomolecule detection has been possible with the use of Metamaterial and metasurface in sensing applications with the progress in the domain of nanophotonics and material science. Even though the progress in biosensing research is expected to continue, there lie challenges along the way. These challenges along the way can be divided into two general categories. The first one is the challenges related to materials and fabrication which include scalable and large-scale fabrication requiring the incorporation of different material platforms. The second one is the physics and engineering challenge incorporating the work on novel concepts, new design development with improved functionalities, and integration of metasurfaces with other materials [225]. These general categories can further be classified into the following sub-categories in terms of the challenges and future perspective.

4.1. Correlation between the simulation and experimental results

An important indicator and facilitator in the progress of biosensing research using these artificial materials is the use of numerical analysis tools such as Lumerical FDTD, COMSOL Multiphysics, and CST Microwave Studio software for the geometrical, optical, and material parameter exploration of the biosensor's performance estimation, evaluation, and comparison. However, from a fabrication point of view, these metamaterials and metasurface-based biosensors are expected to exhibit and verify improved accuracy and sensitivity to correlate with simulated data for the biosensor's sensing evaluation.

4.2. Fabrication challenges and future perspectives

The metasurfaces that are fabricated using planar technology can merge the optics and chip-making process. However, materials used in the research laboratories in metasurface fabrication are incompatible with the industry standards of semiconductor fabrication techniques. Hence, it is challenging to implement metasurface fabrication technology for industry-prepared and scalable manufacturing-like standards. For example, common plasmonic metals (Au, Ag) are incompatible with CMOS fabrication technology [225]. In terms of the design aspect, metasurfaces have made huge progress recently. For example, nano-cylinder meta-atoms have been replaced by high inverse design structures having high performance [226]. Also, the fabrication of large-area metasurfaces which could be pivotal for sensing applications is not free of challenges. Most electron beam lithography tools available in the laboratory cannot pattern large areas [225].

Metamaterials and metasurface-based biosensors have advantages such as high sensitivity and fast detection compared to traditional biosensors. However, the drawbacks include the high cost of processing and low selectivity [227]. Therefore, there should be a balance between cost and sensitivity improvement. It can be expected that top-down lithography approaches (low-cost and large-scale) such as deep and extreme ultra-violet lithography, nanoimprinting, nano stencils, and interference lithography can become significant as alternative manufacturing strategies. However, in the metasurface-based biosensors in the THz region, the thickness of the thin-film analyte goes below 10 nm due to the huge dimensional mismatch between thickness and THz wavelength. Because of the insufficient interaction between the electromagnetic wave and the material, metasurface designs based on traditional photolithography are unable to detect highly subwavelength analytes. Another recent manufacturing technique called atomic layer deposition (ALD) can extend the reach of the metasurface-based biosensing platforms achieving better sensitivities (THz region) that are higher than traditional solutions [228]. For example, slot arrays with widths of 5 and 10 nm and various forms and aspect ratios were successfully created using this approach by Chen et al. in which an unusual field enhancement factor as high as 25,000 was determined from experimental data for a 1 nm nanogap structure during THz characterization [229]. Furthermore, it was expected that by introducing molecules, it would be possible to greatly improve light-matter interaction, which might have a direct use on extremely sensitive sensing systems.

The fabrication of 3D metamaterials requires the creation of 3D meta-atoms termed "metamolecule". Multistep electron beam lithography (EBL) overlay can be used to create these 3D metamolecules at the nanoscale. The procedure is time-consuming and expensive. Direct laser writing (DLW) and photolithography techniques are employed for the successful fabrication of 3D metamolecules. The DLW process can create 3D meta molecules with nanometer-scale dimensions, but there are few options for materials and shapes. The photolithography and EBL overlay processes, on the other hand, provide a wide range of material options through e-beam evaporation, sputtering, and electroplating. However, when compared to the DLW approach, the EBL overlay procedure takes longer and costs more money [24]. In terms of scalability, manufacturing at the scale of a device is not a good fit for the fabrication of

optical metamaterials using focused ion beam milling and electron beam lithography. These procedures have a high cost and low throughput. Large-scale nanofabrication techniques are necessary for commercialization. Techniques like self-assembled monolayers (SAM) and nanoimprint lithography (NIL) can be taken into consideration in this regard [24].

Thermal dewetting (TDW) and glancing angle deposition (GLAD) are two bottom-up nanofabrication processes for creating nanopattern/sculpt thin films. These methods have the benefit of enabling large-scale plasmonic metasurfaces without the use of lithography. TDW and GLAD are used to create quasi-ordered plasmonic metasurfaces, whereas traditional lithographic techniques are used to create high-ordered metasurfaces. The GLAD technique produces nanostructures during the material deposition in a single fabrication step. Meanwhile, the thermal dewetting (TDW) technique creates large-scale metallic nanostructures through post-thermal annealing. GLAD and TDW also aid in the creation of unique, complex, and highly ordered nanostructures with chirality or hyperbolic dispersion for biosensing using traditional lithography [230]. Examples include the detection of human IgG antigen based on the thermal dewetting technique using Au nanoislands [231]. The limit of detection (LoD) of the sensor was estimated to be 1.03 pM and 1.18 pM for gold functionalization and dielectric. Dielectric functionalization protocols had a dynamic range of 1 pM–100 pM. Furthermore, the detection of anti-rIgG binding using the GLAD technique needed Au nano domes in which the sensitivity factor was discovered to be 123 nm/RIU and 27 nM-PBS served as the limit of detection (LoD) [232]. Research works based on the TDW, and GLAD techniques are ongoing [233–240], but these techniques still have a long way to go as different deposition conditions have profound synergistic effects affecting the resulting metasurface.

Hence, these fabrication techniques still need to be improved for use in real-world situations. Scalability and mass production are both issues with top-down fabrication methods. Contrarily, bottom-up methods have restrictions on the controllability, uniformity, and resolution of the manufactured structures. There need to be modifications made to the nanofabrication processes [24].

4.3. Implementation of artificial intelligence

Artificial Intelligence (AI), especially machine learning, has revolutionized many aspects of science and technology. The study of machine learning has sparked great interest among researchers working in biosensing, just like in other fields. The selection of material is an important part of the design of the biosensor. Hence, suitable fabrication methods (top-down or bottom-up approaches) are imperative to obtain different structures, shapes, and geometries for the biosensor design [241–243]. AI-assisted fabrication and characterization techniques for material preparation based on statistics and mathematics are ongoing, realizing the fabrication techniques by AI-assisted systems such as artificial neural network (ANN)-based design parameters. One of the examples includes the prediction of LSPR signal via matching the fabrication parameters and size of the gold (Au) nanoparticles with an ANN model to exhibit the desired properties and physical structures of the AuNPs [241,244–250] The advantages include the rapid analysis of several experimental data for the design of smart materials and their fabrication along with the information on their compositions and properties needed for controllable experimental conditions with high production rate [241].

Based on machine learning algorithms, the behavior of biosensor design with metamaterial integration was used. According to the literature, *meta*-plasmonic structures with machine learning have increased detection sensitivity by more than 13 times [251]. Furthermore, Deep Neural Networks (DNNs) enabled by computer hardware technology advancement led to breakthroughs in autonomous driving, medical diagnosis, drug delivery, and design optimization of structures, among others [252]. In the nanophotonics context, DNNs have been used to face the issue of the inverse design process [253]. For example, Malkeil et al. simulated and trained datasets for bi-directional DNN training for geometry prediction when inputs are in the form of spectra [254]. Vice versa, spectrum predictions are done when geometries are used as inputs. A similar approach was implemented for efficient metasurface [255] and chiral metamaterial [256] design. Herpes virus (simplex) detection was realized from holographic images. However, full utilization has not been done for spectral-based biosensing [257]. Molecular barcodes in unison with DNN can have advancement in the identification and characterization of biological specimens in the real environment [258]. Metastructures have been reverse-engineered in combination with artificial intelligence to achieve molecularly adapted cognition during biosensing and efficiently exploit enhanced electromagnetic field hotspots. As an example, demonstrating the accuracy and utility of neural networks in predicting optical resonances, a simple plasmonic sensor structure was assembled from periodic gold nanodisk arrays. The test results showed that 97.5 % of the predictions had a relative error of less than 5 % over the visible wavelength range, and all-important resonance properties were well preserved. Hence, a well-trained neural network (NN) could accurately predict the spectrum of a myriad of nanostructures within the range of investigated parameters, and each prediction was completed in a few milliseconds. Such tools could provide a general solution for minimizing the cost of plasmonic sensor simulation and guide the design and fabrication of related photonic devices [259].

These next-level metamaterials and metasurfaces' inverse design approaches are still at the beginner level, but they present exciting opportunities and challenges for future research. Such techniques face the deficit of robust protocols for in-situ measurements or limitations in the spectral range. It can be mitigated with the advanced fluid integration scheme [260]. Inverse design can also be implemented for designing 3D photonic devices [261], an approach that can be applied to the metamaterial and metasurface-based biosensor design scheme.

4.4. Technical difficulties in real-life implementation

Looking ahead of the laboratory, the sensor device miniaturization is another approach for the development of field-ready molecular biosensors at a fraction of the cost compared to conventional bulky spectrometers [227]. The need for scalable sensing platforms is the issue with metamaterial-based biosensors for mass production, lowering the cost of fabrication. Plasmonic biosensors can

pave the way for the development of multiplexing capabilities that will allow for the detection of numerous viruses on a single platform [262]. A similar strategy can be realized and put into practice for the metamaterial-based sensors [242]. The sensing devices based on metamaterials must be reliable and repeatable. To make biosensors widely used, a lab-on-a-chip system must also be created. To address the limitations of plasmonic biosensors, research has been conducted on the lab-on-a-chip setup. Metamaterial-based biosensors may employ similar strategies to detect biomolecules more quickly and precisely in the future [242].

For the real-time detection of complex samples, wearable technology can use plasmonic biosensing. Additional steps are still necessary for commercial plasmonic metasurfaces to be used for immediate detection. The challenge of producing plasmon chips on a large scale while keeping costs in check may need to be overcome in the future. Another way to increase detection effectiveness while reducing cost is by selecting a different or novel metamaterial [157].

4.5. New material selection

Utilizing new functional materials (liquid crystals, 2D materials, and phase-change materials), tunable/reconfigurable metasurfaces will produce fascinating and varied functions in a wider range of applications. Metasurfaces with multiple uses can produce near-field enhancement and act as light sources on a chip. By utilizing active materials like GaN and GaAs, these features can be used for the integration of ultra-compact sensors. Other substances, including perovskites and HI chalcogenides, have been used in metasurfaces to create high-performance optical molecular sensors by obtaining distinctive optical features [157]. For commercial applications regarding THz metamaterials/metasurfaces-based sensors, all-polymeric materials with sensing abilities in the THz region can provide promising outcomes with stable, reusable, and low-cost properties [263].

4.6. Clinical assessment

Another point to note is that the metamaterial and metasurface-based biosensing applications in clinical settings must be addressed. The first step will be the verification process, meaning if the biosensors can address the actual clinical need and give critically relevant data. In addition, the safety, reliability, and reproducibility of the equipment must be tested [155].

Therefore, the fabrication challenges related to metamaterial and metasurface-based sensors can be overcome by formulating new material synthesis strategies, fabrication methods, and the design of new material systems. In addition, with the implementation of artificial intelligence (AI) photonics technologies, many hardware fundamental problems can be solved through complex and sophisticated algorithms. This will pave the way for the generation of metamaterial-based sensing devices with excellent performance parameters [264].

5. Conclusion

In principle, in this review, we have discussed the theory, classification, and important findings of biosensing applications related to metamaterials and metasurfaces. Operating frequency region (gigahertz, terahertz, and optical) was the classification criteria's main emphasis. The differences in the biosensing applications in these frequency domains mostly stem from the unique interaction mechanisms and properties at each frequency range. Biosensing in the GHz domain relies on electrical properties and impedance changes, the THz domain focuses on molecular vibrational resonances, and the optical frequency domain is based on surface plasmon resonance. However, overlapping features such as resonant mechanisms and material selection, structure topology (split ring resonator of various configurations), and microfluidic technology were also mentioned in these frequency domains. Metamaterial and metasurfaces are important for the detection of small microorganisms, molecules, and specimens which were not possible with conventional sensors. However, there are challenges in the form of fabrication difficulties, finding a trade-off between sensitivity and cost, and technical difficulties in verifying the simulated and experimental data for the sensor performance is necessary. The new artificial intelligence (AI) optimized, ultra-sensitive metasurfaces can enable the detection and identification of different analytes and their interaction in a complex biological environment for novel, improved, and miniaturized sensing devices by harnessing different aspects of machine learning. The ultimate performance of biosensors involves synergies between bio-interfaces and the converter which is rarely analyzed. Considering this correlation, the corresponding nanostructure design and optimization for maximum performance is intended for biosensing applications. Nevertheless, as challenges and opportunities coexist, the combination of different methodologies will pave a better system for the future of metamaterial and metasurface-based biosensing applications.

Data availability

The datasets used and/or analyzed during the current study are available from the corresponding author upon reasonable request.

CRediT authorship contribution statement

Shadmani Shamim: Writing – original draft, Visualization, Validation, Methodology, Investigation, Formal analysis, Data curation, Conceptualization. **Abu S.M. Mohsin:** Writing – review & editing, Validation, Supervision, Project administration, Investigation, Funding acquisition, Formal analysis, Conceptualization. **Md. Mosaddequr Rahman:** Writing – review & editing, Validation, Supervision, Resources, Project administration, Methodology, Investigation, Funding acquisition. **Mohammed Belal Hossain Bhuian:** Writing – review & editing, Validation, Supervision, Resources, Project administration, Methodology, Funding acquisition.

Declaration of competing interest

The authors declare that they have no known competing financial interests or personal relationships that could have appeared to influence the work reported in this paper.

ACKNOWLEDGMENT

Authors would like to thank Brac University, Bangladesh for the research support.

Appendix A. Supplementary data

Supplementary data to this article can be found online at https://doi.org/10.1016/j.heliyon.2024.e33272.

References

[1] D.J. Smith, W.J. Padilla, D.C. Vier, S. Nemat-Nasser, S. Schultz, Composite medium with simultaneously negative permeability and permittivity, Phys. Rev. Lett. 84 (18) (2000) 4184–4187, https://doi.org/10.1103/physrevlett.84.4184.
[2] C.L. Holloway, E.F. Kuester, J.I. Gordon, J.F. O'Hara, J.T. Booth, D.R. Smith, An overview of the theory and applications of metasurfaces the two-dimensional equivalents of metamaterials, IEEE Antenn. Propag. Mag. 54 (2) (2012) 10–35, https://doi.org/10.1109/map.2012.6230714.
[3] S. Yin, E. Galiffi, A. Alù, Floquet metamaterials, eLight 2 (1) (2022), https://doi.org/10.1186/s43593-022-00015-1.
[4] J. Wen, Q. Ren, P. Ruiguang, H. Yao, Y. Qing, J. Yin, Q. Zhao, Progress in water-based metamaterial absorbers a review, Opt. Mater. Express 12 (4) (2022) 1461, https://doi.org/10.1364/ome.455723.
[5] J.B. Pendry, Metamaterials and the control of electromagnetic fields, in: Conference on Coherence and Quantum Optics, 2007, https://doi.org/10.1364/cqo.2007.cmb2.
[6] C. Caloz, T. Itoh, Transmission line approach of left-handed (LH) materials and microstrip implementation of an artificial LH transmission line, IEEE Trans. Antenn. Propag. 52 (5) (2004) 1159–1166, https://doi.org/10.1109/tap.2004.827249.
[7] R.W. Ziolkowski, E. Heyman, Wave propagation in media having negative permittivity and permeability, Phys. Rev. 64 (5) (2001), https://doi.org/10.1103/physreve.64.056625.
[8] N. Engheta, R.W. Ziolkowski, Metamaterials Physics and Engineering Explorations, Wiley-Interscience, 2006.
[9] Lorentz dispersion model - horiba. (n.d.). Retrieved May 6, 2023, from https://www.horiba.com/fileadmin/uploads/Scientific/Downloads/OpticalSchool_CN/TN/ellipsometer/Lorentz_Dispersion_Model.pdf.
[10] V.G. Veselago, The electrodynamics of substances with simultaneously negative values of ε and μ [in Russian], Usp. Fiz. Nauk 92 (1967) 517–526. English translation in Sov. Phys. Uspekhi, 10, 1968, pp. 509–514.
[11] D.V. Sivukhin, The energy of electromagnetic fields in dispersive media, Opt. Spektrosk. 3 (1957) 308–312 [in Russian].
[12] G.D. Malyuzhinets, A note on the radiation principle, Zh. Tekh. Fiz. 21 (1951) 940–942 [in Russian].
[13] R.A. Silin, "Optical properties of artificial dielectrics (Review) [in Russian], Izv. VUZ Radiofi z. 15 (1972) 809–820, https://doi.org/10.1007/BF01039343. English translation in Radiophys. Quantum Electron., 15, 1972, pp. 615–624.
[14] R.A. Silin, Possibility of creating plane-parallel lenses [in Russian], Opt. Spektrosk. 44 (1978) 189–191. English translation in Opt. Spectrosc., 44, 1978, pp. 109–110.
[15] R.A. Silin, I.P. Chepurnykh, On media with negative dispersion, English translation in J. Commun. Technol. Electron. 46 (2001) 1121–1125 [in Russian], Radiotekh. Elektron., 46, 2001, pp. 1212–1217.
[16] L.I. Mandel'shtam, Lectures on certain problems of oscillation theory lecture 4 [in Russian], Polnoe Sobraniye Trudov, 5, Leningrad, Izdat. Akad. Nauk SSSR (1950) 461–467. also in his Lektsii po Optike Teorii Otnositel'nosti i Kvantovoi Mekhanike, Moscow, Nauka, 1972, pp. 431–437.
[17] L.I. Mandel'shtam, Group velocity in crystalline arrays [in Russian], Zh. Eksp. Teor. Fiz. 15 (1945) 475–478. also in Polnoe Sobraniye Trudov, 2, Leningrad, Izdat. Akad. Nauk SSSR, 1947, pp. 334–338..
[18] H. Lamb, On group-velocity, Proc. London Math. Soc, Ser. 2 (1) (1904) 473–479.
[19] A. Schuster, An Introduction to the Theory of Optics, Edward Arnold, London, 1904, 313-3.
[20] H.C. Pocklington, Growth of a wave-group when the group-velocity is negative, Nature 71 (1852) (1905) 607–608, https://doi.org/10.1038/071607b0.
[21] Y. Liu, X. Zhang, Metamaterials a new frontier of science and technology, Chem. Soc. Rev. 40 (5) (2011) 2494, https://doi.org/10.1039/c0cs00184h.
[22] W. Cai, V.M. Shalaev, Optical metamaterials fundamentals and applications. http://cds.cern.ch/record/1339104/files/978-1-4419-1151-3_BookTOC.pdf, 2009.
[23] N. Yu, F. Capasso, Flat optics with designer metasurfaces, Nat. Mater. 13 (2) (2014) 139–150, https://doi.org/10.1038/nmat3839.
[24] G. Yoon, I. Kim, B. Lee, Challenges in fabrication towards realization of practical metamaterials, Microelectron. Eng. 163 (2016) 7–20, https://doi.org/10.1016/j.mee.2016.05.005.
[25] C.M. Soukoulis, M. Wegener, Past achievements and future challenges in the development of three-dimensional photonic metamaterials, Nat. Photonics 5 (9) (2011) 523–530, https://doi.org/10.1038/nphoton.2011.154.
[26] N. Meinzer, W.L. Barnes, I.R. Hooper, Plasmonic meta-atoms and metasurfaces, Nat. Photonics 8 (12) (2014) 889–898, https://doi.org/10.1038/nphoton.2014.247.
[27] N.I. Zheludev, Y.S. Kivshar, From metamaterials to metadevices, Nat. Mater. 11 (11) (2012) 917–924, https://doi.org/10.1038/nmat3431.
[28] M. Abdollahi, J. Vardaxoglou, W. Whittow, A metasurfaces review definitions and applications, Appl. Sci. 9 (13) (2019) 2727, https://doi.org/10.3390/app9132727.
[29] Z.H. Jiang, S. Yun, L.P. Lin, J.A. Bossard, D.H. Werner, T.S. Mayer, Tailoring dispersion for broadband low-loss optical metamaterials using deep-subwavelength inclusions, Sci. Rep. 3 (1) (2013), https://doi.org/10.1038/srep01571.
[30] S. Tabassum, S. Nayemuzzaman, M. Kala, A.C. Mishra, S. Mishra, Metasurfaces for sensing applications gas, bio and chemical, Sensors 22 (18) (2022) 6896, https://doi.org/10.3390/s22186896.
[31] Y.H. Lee, S. Kim, H. Park, B. Lee, Metamaterials and metasurfaces for sensor applications, Sensors 17 (8) (2017), https://doi.org/10.3390/s17081726.
[32] K. Murugappan, S. Manjunath, Y.M.N.D.Y. Bandara, C.J. Jackson, A. Tricoli, D.N. Neshev, Surface functionalization and texturing of optical metasurfaces for sensing applications, Chem. Rev. 122 (19) (2022) 14990–15030, https://doi.org/10.1021/acs.chemrev.1c00990.
[33] B. Cheng, Y.Z. Ho, Y.C. Lan, D.P. Tsai, Optical hybrid-superlens hyperlens for superresolution imaging, IEEE J. Sel. Top. Quant. Electron. 19 (3) (2013) 4601305, https://doi.org/10.1109/jstqe.2012.2230152.
[34] X. Zhang, Z. Liu, Superlenses to overcome the diffraction limit, Nat. Mater. 7 (6) (2008) 435–441, https://doi.org/10.1038/nmat2141.

[35] P. Mehrotra, B. Chatterjee, S. Sen, EM-wave biosensors A review of RF, microwave, mm-wave and optical sensing, Sensors 19 (5) (2019) 1013, https://doi.org/10.3390/s19051013.
[36] P. Damborský, J. Svitel, J. Katrlík, Optical biosensors, Essays Biochem. 60 (1) (2016) 91–100, https://doi.org/10.1042/ebc20150010.
[37] J.B. Liu, M. Jalali, S. Mahshid, S. Wachsmann-Hogiu, Are plasmonic optical biosensors ready for use in point-of-need applications? Analyst 145 (2) (2020) 364–384, https://doi.org/10.1039/c9an02149c.
[38] J.R. Mejía-Salazar, O.N. Oliveira, Plasmonic biosensing, Chem. Rev. 118 (20) (2018) 10617–10625, https://doi.org/10.1021/acs.chemrev.8b00359.
[39] M. Oliverio, S. Perotto, G. Messina, L.C. Lovato, F. De Angelis, Chemical functionalization of plasmonic surface biosensors A tutorial review on issues, strategies, and costs, ACS Appl. Mater. Interfaces 9 (35) (2017) 29394–29411, https://doi.org/10.1021/acsami.7b01583.
[40] R.T. Hill, Plasmonic biosensors, Wiley Interdisciplinary Reviews-nanomedicine and Nanobiotechnology 7 (2) (2014) 152–168, https://doi.org/10.1002/wnan.1314.
[41] J. Langer, D.J. De Aberasturi, J. Aizpurua, R.A. Alvarez-Puebla, B. Auguié, J.J. Baumberg, G.C. Bazan, S.E.J. Bell, A. Boisen, A.G. Brolo, J. Choo, D. Cialla-May, V. Deckert, L. Fabris, K. Faulds, F.J.G. De Abajo, R. Goodacre, D. Graham, A.J. Haes, L.M. Liz-Marzán, Present and future of surface-enhanced Raman scattering, ACS Nano 14 (1) (2019) 28–117, https://doi.org/10.1021/acsnano.9b04224.
[42] B.D. Gupta, A. Pathak, V. Semwal, Carbon-based nanomaterials for plasmonic sensors A review, Sensors 19 (16) (2019) 3536, https://doi.org/10.3390/s19163536.
[43] M.J. Soler, C.S. Huertas, L.M. Lechuga, Label-free plasmonic biosensors for point-of-care diagnostics a review, Expert Rev. Mol. Diagn. 19 (1) (2018) 71–81, https://doi.org/10.1080/14737159.2019.1554435.
[44] A.V. Zayats, S.A. Maier, Active plasmonics and tuneable plasmonic metamaterials, in: John Wiley & Sons, Inc. eBooks, 2013, https://doi.org/10.1002/9781118634394.
[45] W. Xu, L. Xie, Y. Ying, Mechanisms and applications of terahertz metamaterial sensing a review, Nanoscale 9 (37) (2017) 13864–13878, https://doi.org/10.1039/c7nr03824k.
[46] S. Solinas-Toldo, S. Lampel, S. Stilgenbauer, J. Nickolenko, A. Benner, H. Döhner, T. Cremer, P. Lichter, Matrix-based comparative genomic hybridization Biochips to screen for genomic imbalances, Gene Chromosome Cancer 20 (4) (1997) 399–407, https://doi.org/10.1002/(sici)1098-2264(199712)204.
[47] X. Michalet, A.N. Kapanidis, T.A. Laurence, F. Pinaud, S. Doose, M. Pflughoefft, S. Weiss, The power and prospects of fluorescence microscopies and spectroscopies, Annu. Rev. Biophys. Biomol. Struct. 32 (1) (2003) 161–182, https://doi.org/10.1146/annurev.biophys.32.110601.142525.
[48] S. Webb, S.K. Roberts, S.R. Needham, C.J. Tynan, D.J. Rolfe, M. Winn, D. Clarke, R. Barraclough, M.L. Martin-Fernandez, Single-molecule imaging and fluorescence lifetime imaging microscopy show different structures for high- and low-affinity epidermal growth factor receptors in A431 cells, Biophys. J. 94 (3) (2008) 803–819, https://doi.org/10.1529/biophysj.107.112623.
[49] H. Altug, S.C. Oh, S.A. Maier, J. Homola, Advances and applications of nanophotonic biosensors, Nat. Nanotechnol. 17 (1) (2022) 5–16, https://doi.org/10.1038/s41565-021-01045-5.
[50] J. Homola, Surface plasmon resonance based sensors, in: Springer Series on Chemical Sensors and Biosensors, Springer Nature, 2006, https://doi.org/10.1007/b100321.
[51] Y. Wu, R.D. Tilley, J.J. Gooding, Challenges and solutions in DevelopingUltrasensitive biosensors, J. Am. Chem. Soc. 141 (3) (2019) 1162–1170, https://doi.org/10.1021/jacs.8b09397.
[52] F. Zhou, F. Liu, L. Xiao, K. Cui, X. Feng, W. Zhang, Extending the frequency range of surface plasmon polariton mode with meta-material, Nano-Micro Lett. 9 (1) (2016), https://doi.org/10.1007/s40820-016-0110-8.
[53] A.B. Khanikaev, C. Wu, G. Shvets, Fano-resonant metamaterials and their applications, Nanophotonics 2 (4) (2013) 247–264, https://doi.org/10.1515/nanoph-2013-0009.
[54] Z. Jacob, J.A. Atkinson, Hyperbolic metamaterials fundamentals and applications, Nano Convergence 1 (1) (2014), https://doi.org/10.1186/s40580-014-0014-6.
[55] D. Lee, S. So, G. Hu, M. Kim, T. Badloe, H. Cho, J. Kim, H. Kim, C. Qiu, B. Lee, Hyperbolic metamaterials fusing artificial structures to natural 2D materials, eLight 2 (1) (2022), https://doi.org/10.1186/s43593-021-00008-6.
[56] I.A. Kolmychek, I.V. Malysheva, V. Novikov, A.I. Maydykovskiy, A.P. Leontiev, K.S. Napolskii, T.V. Murzina, Optical properties of hyperbolic metamaterials (brief review), Jetp Letters 114 (11) (2021) 653–664, https://doi.org/10.1134/s0021364021230089.
[57] A. Poddubny, I. Iorsh, P. Belov, Y. Kivshar, Hyperbolic metamaterials, Nat. Photonics 7 (12) (2013) 948–957, https://doi.org/10.1038/nphoton.2013.243.
[58] S.B. Yoo, Q. Park, Metamaterials and chiral sensing a review of fundamentals and applications, Nanophotonics 8 (2) (2019) 249–261, https://doi.org/10.1515/nanoph-2018-0167.
[59] Y.S. Lee, R.M. Kim, S.H. Im, M. Balamurugan, K.T. Nam, Plasmonic metamaterials for chiral sensing applications, Nanoscale 12 (1) (2020) 58–66, https://doi.org/10.1039/c9nr08433a.
[60] K.Y. You, Introductory chapter RF/microwave applications, in: InTech eBooks, 2018, https://doi.org/10.5772/intechopen.73574.
[61] D.M. Sheen, D.L. McMakin, T.D. Hall, Detection of explosives by millimeter-wave imaging, in: Elsevier eBooks, 2007, pp. 237–277, https://doi.org/10.1016/b978-044452204-7/50028-6.
[62] H. Lee, H. Lee, K.H. Yoo, J. Yook, DNA sensing using split-ring resonator alone at microwave regime, J. Appl. Phys. 108 (1) (2010) 014908, https://doi.org/10.1063/1.3459877.
[63] H. Lee, J.P. Lee, H. Moon, I. Jang, J. Choi, J. Yook, H.I. Jung, A planar split-ring resonator-based microwave biosensor for label-free detection of biomolecules, Sensors and Actuators B-chemical 169 (2012) 26–31, https://doi.org/10.1016/j.snb.2012.01.044.
[64] H. Torun, F.C. Top, G. Dundar, An antenna-coupled split-ring resonator for biosensing, J. Appl. Phys. 116 (12) (2014) 124701, https://doi.org/10.1063/1.4896261.
[65] D.J. Smith, J.B. Pendry, M.C.K. Wiltshire, Metamaterials and negative refractive index, Science 305 (5685) (2004) 788–792, https://doi.org/10.1126/science.1096796.
[66] R. Liu, A. Degiron, J.J. Mock, D. Smith, Negative index material composed of electric and magnetic resonators, Appl. Phys. Lett. 90 (26) (2007) 263504, https://doi.org/10.1063/1.2752120.
[67] R.A. Shelby, D.J. Smith, S. Schultz, Experimental verification of a negative index of refraction, Science 292 (5514) (2001) 77–79, https://doi.org/10.1126/science.1058847.
[68] A. Sadeqi, H.R. Nejad, S. Sonkusale, Low-cost metamaterial-on-paper chemical sensor, Opt Express 25 (14) (2017) 16092, https://doi.org/10.1364/oe.25.016092.
[69] A.M.A. Salim, S. Lim, Complementary split-ring resonator-loaded microfluidic ethanol chemical sensor, Sensors 16 (11) (2016) 1802, https://doi.org/10.3390/s16111802.
[70] M. Azab, S.S.A. Obayya, S.S.A. Obayya, Overview of optical biosensors for early cancer detection fundamentals, applications and future perspectives, Biology 12 (2) (2023) 232, https://doi.org/10.3390/biology12020232.
[71] H. Lee, J. Yook, Biosensing using split-ring resonators at microwave regime, Appl. Phys. Lett. 92 (25) (2008) 254103, https://doi.org/10.1063/1.2946656.
[72] H. Lee, H. Lee, K.H. Yoo, J. Yook, DNA sensing using split-ring resonator alone at microwave regime, J. Appl. Phys. 108 (1) (2010) 014908, https://doi.org/10.1063/1.3459877.
[73] H. Lee, J.P. Lee, H. Moon, I. Jang, J. Choi, J. Yook, H.I. Jung, A planar split-ring resonator-based microwave biosensor for label-free detection of biomolecules, Sensors and Actuators B-chemical 169 (2012) 26–31, https://doi.org/10.1016/j.snb.2012.01.044.
[74] K. Jaruwongrungsee, U. Waiwijit, W. Withayachumnankul, T. Maturos, D. Phokaratkul, A. Tuantranont, A. Wisitsoraat, Real-time and label-free biosensing with microfluidic-based split-ring-resonator sensor. https://doi.org/10.1109/nano.2015.7388812, 2015.
[75] S. D, M.P. Jayakrishnan, H.P. Thushara, S. Mridula, P. Mohanan, Microwave based biosensor for blood glucose monitoring. https://doi.org/10.1109/icacc.2015.56, 2015.

[76] B. Camli, E. Kusakci, B. Lafci, S. Salman, H. Torun, Cost-effective, microstrip antenna driven ring resonator microwave biosensor for biospecific detection of glucose, IEEE J. Sel. Top. Quant. Electron. 23 (2) (2017) 404–409, https://doi.org/10.1109/jstqe.2017.2659226.

[77] Y. An, B. Kim, G. Yun, S.W. Kim, S.B. Hong, J. Yook, Flexible non-constrained RF wrist pulse detection sensor based on array resonators, IEEE Transactions on Biomedical Circuits and Systems 10 (2) (2016) 300–308, https://doi.org/10.1109/tbcas.2015.2406776.

[78] Y. An, G. Yun, S.W. Kim, J. Yook, Wrist pulse detection system based on changes in the near-field reflection coefficient of a resonator, IEEE Microw. Wireless Compon. Lett. 24 (10) (2014) 719–721, https://doi.org/10.1109/lmwc.2014.2340584.

[79] C. Liu, M. Wang, L.S. Jang, Microfluidics-based hairpin resonator biosensor for biological cell detection, Sensors and Actuators B-chemical 263 (2018) 129–136, https://doi.org/10.1016/j.snb.2018.01.234.

[80] A.M.A. Salim, S. Kim, D.J. Park, S. Lim, Microfluidic BiosensorBasedonMicrowave substrate-integrated waveguide cavity resonator, J. Sens. (2018) 1–13, https://doi.org/10.1155/2018/1324145, 2018.

[81] Y.I. Abdulkarim, L. Deng, H. Luo, S. Huang, M. Karaaslan, O. Altıntaş, M. Bakir, F.F. Muhammadsharif, H.N. Awl, C. Sabah, K.S.L. Al-Badri, Design and study of a metamaterial based sensor for the application of liquid chemicals detection, J. Mater. Res. Technol. 9 (5) (2020) 10291–10304, https://doi.org/10.1016/j.jmrt.2020.07.034.

[82] S.A. Qureshi, Q.H. Abbasi, A.Y.I. Ashyap, H.A. Majid, M.R. Kamarudin, M. Yue, M.S. Zulkipli, J. Nebhen, Millimetre-wave metamaterial-based sensor for characterisation of cooking oils, Int. J. Antenn. Propag. (2021) 1–10, https://doi.org/10.1155/2021/5520268, 2021.

[83] K. Kuznetsova, V.A. Pashynska, Z.E. Eremenko, Numerical modeling of metal-dielectric metasurface as an element of microwave sensors for biomedical applications, Low Temp. Phys. 50 (1) (2024) 15–20, https://doi.org/10.1063/10.0023885.

[84] M. Bazgir, A. Sheikhi, High Q-Factor Compact Permittivity sensor based on coupled SRR-ELC metamaterial element and Metasurfaces Shield, IEEE Sensor. J. 24 (4) (2024) 4424–4431, https://doi.org/10.1109/jsen.2023.3345477.

[85] A.M.A. Salim, S. Lim, Review of recent metamaterial microfluidic sensors, Sensors 18 (1) (2018) 232, https://doi.org/10.3390/s18010232.

[86] A. Houard, Y. Liu, B. Prade, V. Tikhonchuk, A. Mysyrowicz, Strong enhancement of terahertz radiation from laser filaments in air by a static electric field, Phys. Rev. Lett. 100 (25) (2008), https://doi.org/10.1103/physrevlett.100.255006.

[87] H. Chen, W.J. Padilla, M.J. Cich, A.K. Azad, R.D. Averitt, A.J. Taylor, A metamaterial solid-state terahertz phase modulator, Nat. Photonics 3 (3) (2009) 148–151, https://doi.org/10.1038/nphoton.2009.3.

[88] Y. Sun, P. Du, X. Lu, P. Xie, Z. Qian, S. Fan, Z. Zhu, Quantitative characterization of bovine serum albumin thin-films using terahertz spectroscopy and machine learning methods, Biomed. Opt Express 9 (7) (2018) 2917, https://doi.org/10.1364/boe.9.002917.

[89] F.M. Al-Douseri, Y. Chen, X.Y. Zhang, THz wave sensing for petroleum industrial applications, Int. J. Infrared Millimet. Waves 27 (4) (2007) 481–503, https://doi.org/10.1007/s10762-006-9102-y.

[90] M. Walther, B. Fischer, A. Ortner, A. Bitzer, A. Thoman, H. Helm, Chemical sensing and imaging with pulsed terahertzradiation, Analyticaland BioanalyticalChemistry 397 (3) (2010) 1009–1017, https://doi.org/10.1007/s00216-010-3672-1.

[91] M. Janneh, V. Ferrari, E. Palange, A. Tenggara, D. Byun, Design of a metasurface-based dual-band Terahertz perfect absorber with very high Q-factors for sensing applications, Opt Commun. 416 (2018) 152–159, https://doi.org/10.1016/j.optcom.2018.02.013.

[92] S. Banerjee, C.S. Amith, D. Kumar, G. Damarla, A.K. Chaudhary, S. Goel, B.P. Pal, D.R. Chowdhury, Ultra-thin subwavelength film sensing through the excitation of dark modes in THz metasurfaces, Opt Commun. 453 (2019) 124366, https://doi.org/10.1016/j.optcom.2019.124366.

[93] X. Yan, M. Yang, Z. Zhang, L. Liang, D. Wei, M. Wang, M. Zhang, T. Wang, L. Liu, J. Xie, J. Yao, The terahertz electromagnetically induced transparency-like metamaterials for sensitive biosensors in the detection of cancer cells, Biosens. Bioelectron. 126 (2019) 485–492, https://doi.org/10.1016/j.bios.2018.11.014.

[94] X. Wu, X. Pan, B. Quan, X. Xu, C. Gu, L. Wang, Self-referenced sensing based on terahertz metamaterial for aqueous solutions, Appl. Phys. Lett. 102 (15) (2013) 151109, https://doi.org/10.1063/1.4802236.

[95] Y. Yang, D. Xu, W. Zhang, High-sensitivity and label-free identification of a transgenic genome using a terahertz meta-biosensor, Opt Express 26 (24) (2018) 31589, https://doi.org/10.1364/oe.26.031589.

[96] S.K. Park, S.H. Cha, G. Shin, Y.H. Ahn, Sensing viruses using terahertz nano-gap metamaterials, Biomed. Opt Express 8 (8) (2017) 3551, https://doi.org/10.1364/boe.8.003551.

[97] C. Tang, J. Yang, Y. Wang, J. Cheng, X. Li, C. Chang, J. Hu, J. Lü, Integrating terahertz metamaterial and water nanodroplets for ultrasensitive detection of amyloid β aggregates in liquids, Sensors and Actuators. B, Chemical 329 (2021) 129113, https://doi.org/10.1016/j.snb.2020.129113.

[98] C. Zhang, L. Liang, L. Ding, B. Jin, Y. Hou, C. Li, L. Jiang, W. Liu, W. Hu, Y. Lu, L. Kang, W. Xu, J. Chen, P. Wu, Label-free measurements on cell apoptosis using a terahertz metamaterial-based biosensor, Appl. Phys. Lett. 108 (24) (2016) 241105, https://doi.org/10.1063/1.4954015.

[99] W. Xu, L. Xie, J. Zhu, W. Wang, Z. Ye, Y. Ma, C. Tsai, S. Chen, Y. Ying, Terahertz sensing of chlorpyrifos-methyl using metamaterials, Food Chem. 218 (2017) 330–334, https://doi.org/10.1016/j.foodchem.2016.09.032.

[100] T. Hasebe, S. Kawabe, H. Matsui, H. Tabata, Metallic mesh-based terahertz biosensing of single- and double-stranded DNA, J. Appl. Phys. 112 (9) (2012) 094702, https://doi.org/10.1063/1.4761966.

[101] K. Kashiwagi, L. Xie, X. Li, T. Kageyama, M. Miura, H. Miyashita, J. Kono, S.H. Lee, Flexible and stackable terahertz metamaterials via silver-nanoparticle inkjet printing, AIP Adv. 8 (4) (2018) 045104, https://doi.org/10.1063/1.5006867.

[102] H. Tao, L.R. Chieffo, M.A. Brenckle, S.M. Siebert, M. Liu, A.C. Strikwerda, K. Fan, D.L. Kaplan, X. Zhang, R.D. Averitt, F.G. Omenetto, Metamaterials on paper as a SensingPlatform, Adv. Mater. 23 (28) (2011) 3197–3201, https://doi.org/10.1002/adma.201100163.

[103] B. Ruan, J. Guo, L. Wu, J. Zhu, Q.S. You, X. Dai, Y. Xiang, Ultrasensitive terahertz biosensors based on fano resonance of a graphene/waveguide hybrid structure, Sensors 17 (8) (2017) 1924, https://doi.org/10.3390/s17081924.

[104] Z.S. Tabatabaeian, Developing THz metasurface with array rectangular slot with High Q-factor for early skin cancer detection, Optik 264 (2022) 169400, https://doi.org/10.1016/j.ijleo.2022.169400.

[105] R. Cheng, L. Xu, X. Yu, L. Zou, Y. Shen, X. Deng, High-sensitivity biosensor for identification of protein based on terahertz Fano resonance metasurfaces, Opt Commun. 473 (2020) 125850, https://doi.org/10.1016/j.optcom.2020.125850.

[106] C. Zhang, L. Liang, L. Ding, B. Jin, Y. Hou, C. Li, L. Jiang, W. Liu, W. Hu, Y. Lu, L. Kang, W. Xu, J. Chen, P. Wu, Label-free measurements on cell apoptosis usinga terahertz metamaterial-based biosensor, Appl. Phys. Lett. 108 (24) (2016) 241105, https://doi.org/10.1063/1.4954015.

[107] K. Yang, J. Li, M.L. De La Chapelle, G. Huang, Y. Wang, J. Zhang, D. Xu, J. Yao, X. Yang, W. Fu, A terahertz metamaterial biosensor for sensitive detection of microRNAs based on gold-nanoparticles and strand displacement amplification, Biosens. Bioelectron. 175 (2021) 112874, https://doi.org/10.1016/j.bios.2020.112874.

[108] I. Al-Naib, Biomedical sensing with conductively coupled terahertz metamaterial resonators, IEEE J. Sel. Top. Quant. Electron. 23 (4) (2017) 1–5, https://doi.org/10.1109/jstqe.2016.2629665.

[109] A. Ahmadivand, B. Gerislioglu, A.A. Orouji, A. Kaushik, P. Manickam, S.A. Ghoreishi, Functionalized terahertz plasmonic metasensors Femtomolar-level detection of SARS-CoV-2spike proteins, Biosens. Bioelectron. 177 (2021) 112971, https://doi.org/10.1016/j.bios.2021.112971.

[110] S.K. Park, J. Hong, S. Choi, H. Kim, W. Park, S.W. Han, J. Park, S.H. Lee, D. Kim, Y.H. Ahn, Detection of microorganisms using terahertz metamaterials, Sci. Rep. 4 (1) (2015), https://doi.org/10.1038/srep04988.

[111] Y. Li, X. Chen, F. Hu, D. Li, H. Teng, Q. Rong, W. Zhang, J. Han, H. Liang, Four resonators based high sensitive terahertz metamaterial biosensor used for measuring concentration of protein, J. Phys. D 52 (9) (2019) 095105, https://doi.org/10.1088/1361-6463/aaf7e9.

[112] K. Liu, R. Zhang, Y. Liu, X. Chen, K. Li, E. Pickwell-MacPherson, Gold nanoparticle enhanced detection of EGFR with a terahertz metamaterial biosensor, Biomed. Opt Express 12 (3) (2021) 1559, https://doi.org/10.1364/boe.418859.

[113] Y.J. Lee, S.H. Lee, J. Kwak, H.K. Song, M. Seo, Detection and discrimination of SARS-CoV-2 spike protein-derived peptides using THz metamaterials, Biosens. Bioelectron. 202 (2022) 113981, https://doi.org/10.1016/j.bios.2022.113981.

[114] A. Ahmadivand, B. Gerislioglu, A. Tomitaka, P. Manickam, A. Kaushik, S. Bhansali, M. Nair, N. Pala, Extreme sensitive metasensor for targeted biomarkers identification using colloidal nanoparticles-integrated plasmonic unit cells, Biomed. Opt Express 9 (2) (2018) 373, https://doi.org/10.1364/boe.9.000373.

[115] S. Shen, X. Liu, Y. Shen, J. Qu, E. Pickwell-MacPherson, X. Wei, Y. Sun, Recent advances in the development of materials for terahertz metamaterial sensing, Adv. Opt. Mater. 10 (1) (2021) 2101008, https://doi.org/10.1002/adom.202101008.

[116] P. Wan, X. Wen, C. Sun, B.K. Chandran, H. Zhang, X. Sun, X.D. Chen, Flexible transparent films based on nanocomposite networks of polyaniline and carbon nanotubes for high-performance gas sensing, Small 11 (40) (2015) 5409–5415, https://doi.org/10.1002/smll.201501772.

[117] S. Yang, W. Chen, W. Chen, W. Jin, J. Zhou, H. Zhang, G.S. Zakharova, High sensitivity and good selectivity of ultralong MoO3 nanobelts for trimethylamine gas, Sensors and Actuators B-chemical 226 (2016) 478–485, https://doi.org/10.1016/j.snb.2015.12.005.

[118] A. Mazinani, J. Nine, R. Chiesa, G. Candiani, P. Tarsini, T.T. Tung, D. Losic, Graphene oxide (GO) decorated on multi-structured porous titania fabricated byplasma electrolytic oxidation (PEO) for enhanced antibacterial performance, Mater. Des. 200 (2021) 109443, https://doi.org/10.1016/j.matdes.2020.109443.

[119] M.A. Shathi, M. Chen, N.A. Khoso, M.T. Rahman, B. Bhattacharjee, Graphene coated textile based highlyflexible and washable sportsbra for human health monitoring, Mater. Des. 193 (2020) 108792, https://doi.org/10.1016/j.matdes.2020.108792.

[120] Y.S. Chen, J. Ren, Y. Sun, W. Liu, X. Lu, S. Guan, Efficacy of graphene nanosheets on the plasma sprayed hydroxyapatite coating Improved strength, toughness and in-vitro bio performance with osteoblast, Mater. Des. 203 (2021) 109585, https://doi.org/10.1016/j.matdes.2021.109585.

[121] Z. Vafapour, Y. Hajati, M. Hajati, H. Ghahraloud, Graphene-based mid-infrared biosensor, J. Opt. Soc. Am. B 34 (12) (2017) 2586, https://doi.org/10.1364/josab.34.002586.

[122] A. Keshavarz, A. Zakery, Ultrahigh sensitive temperature sensor based on graphene-semiconductor metamaterial, Appl. Phys. A 123 (12) (2017), https://doi.org/10.1007/s00339-017-1399-y.

[123] M. Esfandiyari, M. Norouzi, P. Haghdoust, S. Jarchi, Study of a surface plasmon resonance OpticalFiberSensor basedon PeriodicallyGratingand graphene, Silicon 10 (6) (2018) 2711–2716, https://doi.org/10.1007/s12633-018-9810-7.

[124] P. Kachroo, A. Dominic, Influence of chemical potential on graphene-based SPR sensor's performance, IEEE Photon. Technol. Lett. 30 (1) (2018) 95–98, https://doi.org/10.1109/lpt.2017.2776945.

[125] X. Chen, W. Fan, C. Song, Multiple plasmonic resonance excitations on graphene metamaterials for ultrasensitive terahertz sensing, Carbon 133 (2018) 416–422, https://doi.org/10.1016/j.carbon.2018.03.051.

[126] D. Hu, T. Li, B. Zeng, H. Zhang, H. Lv, X. Huang, W. Zhang, A.K. Azad, A graphene based tunable terahertz sensor with double Fano resonances, Nanoscale 7 (29) (2015) 12682–12688, https://doi.org/10.1039/c5nr03044g.

[127] J. Tang, Y. Ye, J. Xu, Z. Zheng, X. Jin, L. Jiang, J. Jiang, Y. Xiang, High-sensitivity terahertz refractive index sensor in a multilayered structure with graphene, Nanomaterials 10 (3) (2020) 500, https://doi.org/10.3390/nano10030500.

[128] S. Xu, J. Zhan, B. Man, S. Jiang, W. Yue, S. Gao, C. Guo, H. Liu, Z. Li, J. Wang, Y. Zhou, Real-time reliable determination of binding kinetics of DNA hybridization using a multi-channel graphene biosensor, Nat. Commun. 8 (1) (2017), https://doi.org/10.1038/ncomms14902.

[129] W. Xu, L. Xie, J. Zhu, L. Tang, R. Singh, C. Wang, Y. Ma, H. Chen, Y. Ying, Terahertz biosensing with a graphene-metamaterial heterostructure platform, Carbon 141 (2019) 247–252, https://doi.org/10.1016/j.carbon.2018.09.050.

[130] S.Y. Lee, J. Choe, C. Kim, S. Bae, J. Kim, Q. Park, M. Seo, Graphene assisted terahertz metamaterials for sensitive bio-sensing, Sensors and Actuators B-chemical 310 (2020) 127841, https://doi.org/10.1016/j.snb.2020.127841.

[131] X. Guo, H. Hu, X. Zhu, X. Yang, Q. Dai, Higher order Fano graphene metamaterials for nanoscale optical sensing, Nanoscale 9 (39) (2017) 14998–15004, https://doi.org/10.1039/c7nr05919a.

[132] Z. Yi, C. Liang, X. Chen, Z. Zhou, Y. Tang, X. Ye, Y. Yi, J. Wang, P. Wu, Dual-band plasmonic perfect absorber based on graphene metamaterials for refractive index sensing application, Micromachines 10 (7) (2019) 443, https://doi.org/10.3390/mi10070443.

[133] K. Li, X. Ma, Z. Zhang, J. Song, Y. Xu, G. Song, Sensitive refractive index sensing with tunable sensing range and good operation angle-polarization-tolerance using graphene concentric ring arrays, J. Phys. D 47 (40) (2014) 405101, https://doi.org/10.1088/0022-3727/47/40/405101.

[134] J. Huang, G. Niu, Z. Yi, X. Chen, Z. Zhou, X. Ye, Y. Tang, Y. Yi, T. Duan, Y. Yi, High sensitivity refractive index sensing with good angle and polarization tolerance using elliptical nanodisk graphene metamaterials, Phys. Scripta 94 (8) (2019) 085805, https://doi.org/10.1088/1402-4896/ab185f.

[135] S. Gong, B. Xiao, L. Xiao, S. Tong, S. Xiao, X. Wang, Hybridization-induced dual-band tunable graphene metamaterials for sensing, Opt. Mater. Express 9 (1) (2019) 35, https://doi.org/10.1364/ome.9.000035.

[136] A. Hamouleh-Alipour, A. Mir, A. Farmani, Analytical modeling and design of a graphene metasurface sensor for thermo-optical detection of terahertz plasmons, IEEE Sensor. J. 21 (4) (2021) 4525–4532, https://doi.org/10.1109/jsen.2020.3035577.

[137] X. Du, F. Yan, W. Wang, L. Zhang, Z. Bai, H. Zhou, Y. Hou, Thermally-stable graphene metamaterial absorber with excellent tunability for high-performance refractive index sensing in the terahertz band, Opt. Laser Technol. 144 (2021) 107409, https://doi.org/10.1016/j.optlastec.2021.107409.

[138] R. Wang, L. Xie, S. Hameed, C. Wang, Y. Ying, Mechanisms and applications of carbon nanotubes in terahertz devices A review, Carbon 132 (2018) 42–58, https://doi.org/10.1016/j.carbon.2018.02.005.

[139] X. He, W. Gao, Q. Zhang, L. Ren, J. Kono, Carbon-based terahertz devices. https://doi.org/10.1117/12.2185159, 2015.

[140] R. Wang, W. Xu, L. Xie, Y. Ying, Millimeter, and terahertz waves (IRMMW-THz 2019), in: 2019 44th International Conference on Infrared, IEEE, Paris, France, 2019, pp. 1202–1203, https://doi.org/10.1109/irmmw-thz.2019.8873844 [IRMMW-THz 2019 Future Events]. (2019).

[141] J. Shi, Z. Li, D.K. Sang, Y. Xiang, J. Li, S. Zhang, H. Zhang, THz photonics in two dimensional materials and metamaterials properties, devices and prospects, J. Mater. Chem. C 6 (6) (2018) 1291–1306, https://doi.org/10.1039/c7tc05460b.

[142] Z. Liu, K. Aydin, Localized surface plasmons in nanostructured monolayer black phosphorus, Nano Lett. 16 (6) (2016) 3457–3462, https://doi.org/10.1021/acs.nanolett.5b05166.

[143] Q. Fo, L. Pan, X. Chen, Q. Xu, C. Ouyang, X. Zhang, Z. Tian, Y. Li, L. Liu, J. Han, W. Zhang, Anisotropic plasmonic response of black phosphorus nanostrips in terahertz metamaterials, IEEE Photon. J. 10 (3) (2018) 1–9, https://doi.org/10.1109/jphot.2018.2842059.

[144] I. Staude, J. Schilling, Metamaterial-inspired silicon nanophotonics, Nat. Photonics 11 (5) (2017) 274–284, https://doi.org/10.1038/nphoton.2017.39.

[145] X. Zhao, Y. Wang, J. Schalch, G. Duan, K. Cremin, J. Zhang, C. Chen, R.D. Averitt, X. Zhang, Optically modulated ultra-broadband all-silicon metamaterial terahertz absorbers, ACS Photonics 6 (4) (2019) 830–837, https://doi.org/10.1021/acsphotonics.8b01644.

[146] Y. Wang, D. Zhu, Z. Cui, L. Hou, L. Lin, Q. Fangfang, X. Liu, P. Nie, All-dielectric terahertz plasmonic metamaterial absorbers and high-sensitivity sensing, ACS Omega 4 (20) (2019) 18645–18652, https://doi.org/10.1021/acsomega.9b02506.

[147] W. Xu, L. Xie, J. Zhu, L. Tang, R. Singh, C. Wang, Y. Ma, H. Chen, Y. Ying, Terahertz biosensing with a graphene-metamaterial heterostructure platform, Carbon 141 (2019) 247–252, https://doi.org/10.1016/j.carbon.2018.09.050.

[148] W. Xu, L. Xie, J. Zhu, X. Xu, Z. Ye, C. Wang, Y. Ma, Y. Ying, Gold nanoparticle-based terahertz metamaterial sensors mechanisms and applications, ACS Photonics 3 (12) (2016) 2308–2314, https://doi.org/10.1021/acsphotonics.6b00463.

[149] S. Zeng, R. Singh, J. Shang, T. Yu, C. Chen, F. Yin, D. Baillargeat, P. Coquet, H. Ho, A.V. Kabashin, K. Yong, Graphene-gold metasurface architectures for ultrasensitive PlasmonicBiosensing, Adv. Mater. 27 (40) (2015) 6163–6169, https://doi.org/10.1002/adma.201501754.

[150] M.G. Amin, M. Farhat, H. Bağcı, A dynamically reconfigurable Fano metamaterial through graphene tuning for switching and sensing applications, Sci. Rep. 3 (1) (2013), https://doi.org/10.1038/srep02105.

[151] H. Tian, G. Huang, F. Xie, W. Fu, N. And, X. Yang, THz biosensing applications for clinical laboratories Bottlenecks and strategies, Trends Anal. Chem. 163 (2023) 117057, https://doi.org/10.1016/j.trac.2023.117057.

[152] X. Chen, W. Yang, Z. Wang, J. Li, M. Hu, J. An, Q. Wu, Z. Wang, H. Chen, Y. Wei, H. Du, D. Wang, Improving new particle formation simulation by coupling a volatility-basis set (VBS) organic aerosol module in NAQPMS+APM, Atmos. Environ. 204 (2019) 1–11, https://doi.org/10.1016/j.atmosenv.2019.01.053.

[153] R. Zhou, C. Wang, Y. Huang, K. Huang, Y. Wang, W. Xu, L. Xie, Y. Ying, Label-free terahertz microfluidic biosensor for sensitive DNA detection using graphene-metasurface hybridstructures, Biosens. Bioelectron. 188 (2021) 113336, https://doi.org/10.1016/j.bios.2021.113336.

[154] K. Jaruwongrungsee, U. Waiwijit, W. Withayachumnankul, T. Maturos, D. Phokaratkul, A. Tuantranont, W. Wlodarski, A. Martucci, A. Wisitsoraat, Microfluidic-based split-ring-resonator sensor for real-time and label-free biosensing, Procedia Eng. 120 (2015) 163–166, https://doi.org/10.1016/j.proeng.2015.08.595.

[155] R. Zhang, Q. Chen, K. Liu, Z. Chen, K. Li, X. Zhang, J. Xu, E. Pickwell-MacPherson, Terahertz microfluidic metamaterial biosensor for sensitive detection of small-volume liquid samples, IEEE Transactions on Terahertz Science and Technology 9 (2) (2019) 209–214, https://doi.org/10.1109/tthz.2019.2898390.

[156] Z. Geng, X. Zhang, Z. Fan, X. Lv, H. Chen, A route to terahertz metamaterial biosensor integrated with microfluidics for liver cancer biomarker testing in early stage, Sci. Rep. 7 (1) (2017), https://doi.org/10.1038/s41598-017-16762-y.

[157] S.A. Khan, N.M. Khan, Y. Xie, M. Abbas, M. Rauf, I. Mehmood, M. Runowski, S. Agathopoulos, J. Zhu, Optical sensing by metamaterials and metasurfaces from physics to biomolecule detection, Adv. Opt. Mater. 10 (18) (2022) 2200500, https://doi.org/10.1002/adom.202200500.

[158] G.E. Stillman, Optoelectronics, in: Elsevier eBooks, 2002, pp. 21–31, https://doi.org/10.1016/b978-075067291-7/50023-6.

[159] J.N. Jackson, N.J. Halas, Surface-enhanced Raman scattering on tunable plasmonic nanoparticle substrates, Proceedings of the National Academy of Sciences of the United States of America 101 (52) (2004) 17930–17935, https://doi.org/10.1073/pnas.0408319102.

[160] J.N. Anker, W.P. Hall, O. Lyandres, N.C. Shah, J. Zhao, R.P. VanDuyne, Biosensing with plasmonic nanosensors, in: Co-Published with Macmillan Publishers Ltd, UK eBooks, 2009, pp. 308–319, https://doi.org/10.1142/9789814287005_0032.

[161] K. Li, X. Li, M.I. Stockman, D.J. Bergman, Surface plasmon amplification by stimulated emission in nanolenses, Phys. Rev. B 71 (11) (2005), https://doi.org/10.1103/physrevb.71.115409.

[162] Z. Wang, J. Chen, S.A. Khan, F. Li, J. Shen, Q. Duan, X. Liu, J. Zhu, Plasmonic metasurfaces for medical diagnosis applications A review, Sensors 22 (1) (2021) 133, https://doi.org/10.3390/s22010133.

[163] S.M. Predabon, P.H.M. Buzzetti, J.V. Visentainer, E. Radovanovic, J.P. Monteiro, E.M. Girotto, Detection of tumor necrosis factor-alpha cytokine from the blood serum of a rat infected with Pb18 by a gold nanohole array-based plasmonic biosensor, Journal ofNanophotonics 14 (3) (2020) 1, https://doi.org/10.1117/1.jnp.14.036004.

[164] Y. Khan, A. Li, L. Chang, L. Li, L. Guo, Gold nano disks arrays for localized surface plasmon resonance based detection of PSA cancer marker, Sensors and Actuators B-chemical 255 (2018) 1298–1307, https://doi.org/10.1016/j.snb.2017.08.118.

[165] B. Gallinet, O.J.F. Martin, *Ab initio* theory of Fano resonances in plasmonic nanostructures and metamaterials, Phys. Rev. B 83 (23) (2011), https://doi.org/10.1103/physrevb.83.235427.

[166] M.F. Limonov, M.V. Rybin, A.N. Poddubny, Y.S. Kivshar, Fano resonances in photonics, Nat. Photonics 11 (9) (2017) 543–554, https://doi.org/10.1038/nphoton.2017.142.

[167] B. Gallinet, O.J.F. Martin, Relation between near–field and far–field properties of plasmonic Fano resonances, Opt Express 19 (22) (2011) 22167, https://doi.org/10.1364/oe.19.022167.

[168] W. Zhao, D. Ju, Y. Jiang, Sharp FanoResonance within Bi-periodic silver particle array and its application as plasmonic sensor with ultra-high figure of merit, Plasmonics 10 (2) (2015) 469–474, https://doi.org/10.1007/s11468-014-9829-6.

[169] D. Bosomtwi, V.E. Babicheva, Beyond conventional sensing hybrid plasmonic metasurfaces and bound states in the continuum, Nanomaterials 13 (7) (2023) 1261, https://doi.org/10.3390/nano13071261.

[170] M. Bazgir, F.B. Zarrabi, S. Sim, K. Pedram, The nano aperture in optical regime for bio-sensing, metasurface, and energy harvesting application Technical review, Sensors and Actuators. A, Physical 359 (2023) 114495, https://doi.org/10.1016/j.sna.2023.114495.

[171] R.a.M. Lameirinhas, J.P.N. Torres, A. Baptista, A sensor based on nanoantennas, Applied Sciences 10 (19) (2020) 6837. https://doi.org/10.3390/app10196837.

[172] E. Aslan, M. Türkmen, Refractive index sensing characteristics of dual resonances in rectangular fractal nano-apertures, Opt. Mater. 46 (2015) 423–428, https://doi.org/10.1016/j.optmat.2015.04.058.

[173] AE Cetin, S Kaya, A Mertiri, E Aslan, S Erramilli, H Altug, M Turkmen, Dual-band plasmonic resonator based on Jerusalem cross-shaped nanoapertures, Photonics and Nanostructures-Fundamentals and Applications, 2015 Jun 1, pp. 73–80, https://doi.org/10.1016/j.photonics.2015.04.001, 15.

[174] M. Türkmen, S. Aksu, A.E. Çetin, A.A. Yanik, H. Altug, Multi-resonant metamaterials based on UT-shaped nano-aperture antennas, Opt Express 19 (8) (2011) 7921, https://doi.org/10.1364/oe.19.007921.

[175] F.B. Zarrabi, M. Bazgir, S. Ebrahimi, A.S. Arezoomand, Fano resonance for U-I nano-array independent to the polarization providing bio-sensing applications, J. Electromagn. Waves Appl. 31 (14) (2017) 1444–1452, https://doi.org/10.1080/09205071.2017.1351401.

[176] F.B. Zarrabi, S. Sharma, S. Ebrahimi, P.K. Singh, Developing checkerboard cross element metasurface with multi-Fano response for sensing in the infrared spectrum, Opt Commun. 552 (2024) 130060, https://doi.org/10.1016/j.optcom.2023.130060.

[177] Z.S. Tabatabaeian, F. Kazemi, S. Ebrahimi, Plasmonic fractal Metasurface with Fano response for virus detection in the optical spectrum, Opt. Mater. 150 (2024) 115153, https://doi.org/10.1016/j.optmat.2024.115153.

[178] C.F. Kenworthy, L. Stoevelaar, A.J. Alexander, G. Gerini, Using the near field optical trapping effect of a dielectric metasurface to improve SERS enhancement for virus detection, Sci. Rep. 11 (1) (2021), https://doi.org/10.1038/s41598-021-85965-1.

[179] A. Nazary, S. Ebrahimi, A.S. Arezoomand, Design nano cluster high Q-factor perfect plasmonic absorber for bacteria detection in the optical range, Optik 300 (2024) 171652, https://doi.org/10.1016/j.ijleo.2024.171652.

[180] S. Poorgholam-Khanjari, Z. Razavi, F.B. Zarrabi, Reconfigurable optical rectangular particle array absorber based on metal–DNA–metal structure as a refractive index sensor and optical switch, Opt Commun. 489 (2021) 126866, https://doi.org/10.1016/j.optcom.2021.126866.

[181] G.A. Khan, Y. Lü, P. Wang, Plasmon-Enhanced refractive index sensing of biomolecules based on Metal–Dielectric–Metal metasurface in the infrared regime, ACS Omega (2023), https://doi.org/10.1021/acsomega.3c07809.

[182] R. Negahdari, E. Rafiee, Z. Kordrostami, E. Rafiee, Sensitive MIM plasmonic biosensors for detection of hemoglobin, creatinine and cholesterol concentrations, Diam. Relat. Mater. 136 (2023) 110029, https://doi.org/10.1016/j.diamond.2023.110029.

[183] N.A. Salama, S. Obayya, S.M. Alexeree, M.A. Swillam, Ultrasensitive biosensor using a Fano resonant asymmetric all-dielectric metasurface, Proceedings 12568 (2023) 1256818, https://doi.org/10.1117/12.2665763. *Metamaterials XIV*.

[184] H. Chen, X. Fan, W. Fang, B. Zhang, S. Cao, Q. Sun, D. Wang, H. Niu, C. Li, X. Wei, C. Bai, S. Kumar, High-Q Fano resonances in all-dielectric metastructures for enhanced optical biosensing applications, Biomed. Opt Express 15 (1) (2023) 294, https://doi.org/10.1364/boe.510149.

[185] B. Luk'yanchuk, N.I. Zheludev, S.A. Maier, N.J. Halas, P. Nordlander, H. Giessen, C.T. Chong, The Fano resonance in plasmonic nanostructures and metamaterials, Nat. Mater. 9 (9) (2010) 707–715, https://doi.org/10.1038/nmat2810.

[186] G.V. Naik, V.M. Shalaev, A. Boltasseva, Alternative plasmonic materials beyond gold and silver, Adv. Mater. 25 (24) (2013) 3264–3294, https://doi.org/10.1002/adma.201205076.

[187] A. Christ, Y. Ekinci, H.H. Solak, N.A. Gippius, S.G. Tikhodeev, O.J.F. Martin, Controlling the Fano interference in a plasmonic lattice, Phys. Rev. B 76 (20) (2007), https://doi.org/10.1103/physrevb.76.201405.

[188] Q. Li, X. Wu, Y.J. Zhou, Plasmonic nanosensors and metasensors based on new physical mechanisms, Chemosensors 10 (10) (2022) 397, https://doi.org/10.3390/chemosensors10100397.

[189] A. Kiselev, J. Kim, O.J.F. Martin, Mind the gap between theory and experiment, arXiv (Cornell University) (2022), https://doi.org/10.48550/arxiv.2210.14747.

[190] A.E. Miroshnichenko, S. Flach, Y.S. Kivshar, Fano resonances in nanoscale structures, Rev. Mod. Phys. 82 (3) (2010) 2257–2298, https://doi.org/10.1103/revmodphys.82.2257.

[191] M. Rahmani, B. Luk'yanchuk, M. Hong, Fano resonance in novel plasmonic nanostructures, Laser Photon. Rev. 7 (3) (2013) 329–349, https://doi.org/10.1002/lpor.201200021.

[192] P. Athe, S.K. Srivastava, K.B. Thapa, Electromagnetically induced reflectance and Fano resonance in one dimensional superconducting photonic crystal, Physica C-superconductivity and Its Applications 547 (2018) 36–40, https://doi.org/10.1016/j.physc.2018.01.009.

[193] H. Liu, G. Li, K. Li, S. Chen, S. Zhu, C.T. Chan, K.W. Cheah, Linear and nonlinear Fano resonance on two-dimensional magnetic metamaterials, Phys. Rev. B 84 (23) (2011), https://doi.org/10.1103/physrevb.84.235437.

[194] S. Mun, H. Yun, C. Choi, S. Kim, B. Lee, Enhancement and switching of fano resonance in metamaterial, Adv. Opt. Mater. 6 (17) (2018) 1800545, https://doi.org/10.1002/adom.201800545.

[195] S. Mun, C. Choi, J. Hong, B. Lee, Broadband wavelength demultiplexer using Fano-resonant metasurface, Nanophotonics 9 (5) (2020) 1015–1022, https://doi.org/10.1515/nanoph-2019-0492.

[196] L.Q. Chen, N. Xu, L. Singh, T.J. Cui, R. Singh, Y. Zhu, W. Zhang, Defect-induced fano resonances in corrugated plasmonic metamaterials, Adv. Opt. Mater. 5 (8) (2017) 1600960, https://doi.org/10.1002/adom.201600960.

[197] P. Wang, A.V. Krasavin, L. Liu, Y. Jiang, Z. Li, X. Guo, L. Tong, A.V. Zayats, Molecular plasmonics with metamaterials, Chem. Rev. 122 (19) (2022) 15031–15081, https://doi.org/10.1021/acs.chemrev.2c00333.

[198] N. Liu, T.G. Weiss, M. Mesch, L. Langguth, U. Eigenthaler, M. Hirscher, C. Sönnichsen, H. Giessen, Planar metamaterial analogue of electromagnetically induced transparency for plasmonic sensing, Nano Lett. 10 (4) (2010) 1103–1107, https://doi.org/10.1021/nl902621d.

[199] A.E. Cetin, H. Altug, Fano resonant ring/disk plasmonic nanocavities on conducting substrates for advanced biosensing, ACS Nano 6 (11) (2012) 9989–9995, https://doi.org/10.1021/nn303643w.

[200] A.A. Yanik, A.E. Cetin, M. Huang, A. Artar, S.M. Mousavi, A.B. Khanikaev, J.M. Connor, G. Shvets, H. Altug, Seeing protein monolayers with naked eye through plasmonic Fano resonances, Proceedings of the National Academy of Sciences of the United States of America 108 (29) (2011) 11784–11789, https://doi.org/10.1073/pnas.1101910108.

[201] Y. Shen, J. Zhou, T. Liu, Y. Tao, R. Jiang, L. Mingxuan, G. Xiao, J. Zhu, Z. Zhou, X. Wang, C. Jin, J. Wang, Plasmonic gold mushroom arrays with refractive index sensing figures of merit approaching the theoretical limit, Nat. Commun. 4 (1) (2013), https://doi.org/10.1038/ncomms3381.

[202] G. Palermo, R. Singh, N. Maccaferri, G.E. Lio, G. Nicoletta, F. De Angelis, M. Hinczewski, G. Strangi, Hyperbolic dispersion metasurfaces for molecular biosensing, Nanophotonics 10 (1) (2020) 295–314, https://doi.org/10.1515/nanoph-2020-0466.

[203] J.C. Garnett, J. Larmor, Colours in metal glasses and in metallic films, Proc. Roy. Soc. Lond. 73 (488–496) (1904) 443–445, https://doi.org/10.1098/rspl.1904.0058.

[204] R. Singh, Y. Alapan, M. ElKabbash, A.M. Wen, E. Ilker, M. Hinczewski, U.A. Gurkan, N.F. Steinmetz, G. Strangi, Enhancing the angular sensitivity of plasmonic sensors using hyperbolic metamaterials, Adv. Opt. Mater. 4 (11) (2016) 1767–1772, https://doi.org/10.1002/adom.201600448.

[205] N. Vasilantonakis, G.A. Wurtz, V.A. Podolskiy, A.V. Zayats, Refractive index sensing with hyperbolic metamaterials strategies for biosensing and nonlinearity enhancement, Opt Express 23 (11) (2015) 14329, https://doi.org/10.1364/oe.23.014329.

[206] A.V. Kabashin, P.G. Evans, S. Pastkovsky, W. Hendren, G.A. Wurtz, R. Atkinson, R. Pollard, V.A. Podolskiy, A.V. Zayats, Plasmonic nanorod metamaterials for biosensing, Nat. Mater. 8 (11) (2009) 867–871, https://doi.org/10.1038/nmat2546.

[207] R. Yan, T. Wang, X. Yue, H. Wang, Y. Zhang, P. Xu, L. Wang, W. Yuandong, J. Zhang, Highly sensitive plasmonic nanorod hyperbolic metamaterial biosensor, Photon. Res. 10 (1) (2021) 84, https://doi.org/10.1364/prj.444490.

[208] J. McPhillips, A. Murphy, M. Jonsson, W. Hendren, R.R. Atkinson, F. Höök, A.V. Zayats, R. Pollard, High-performance biosensing using arrays of plasmonic nanotubes, ACS Nano 4 (4) (2010) 2210–2216, https://doi.org/10.1021/nn9015828.

[209] A.W. Murphy, Y. Sonnefraud, A.V. Krasavin, P. Ginzburg, F. Morgan, J. McPhillips, G.A. Wurtz, S.F. Maier, A.V. Zayats, R. Pollard, Fabrication and optical properties of large-scale arrays of gold nanocavities based on rod-in-a-tube coaxials, Appl. Phys. Lett. 102 (10) (2013) 103103, https://doi.org/10.1063/1.4794935.

[210] R. Singh, Y. Alapan, M. ElKabbash, E. Ilker, M. Hinczewski, U.A. Gurkan, A. De Luca, G. Strangi, Extreme sensitivity biosensing platform based on hyperbolic metamaterials, Nat. Mater. 15 (6) (2016) 621–627, https://doi.org/10.1038/nmat4609.

[211] S. Hu, Y. Chen, Y. Chen, L. Chen, H. Zheng, N.H. Azeman, M. Liu, G. Liu, Y. Luo, Z. Chen, High-performance fiber plasmonic sensor by engineering the dispersion of hyperbolic metamaterials composed of Ag/TiO2, Opt Express 28 (17) (2020) 25562, https://doi.org/10.1364/oe.397461.

[212] C. Li, J. Gao, M. Shafi, R. Liu, Z. Zha, D. Feng, M. Liu, X. Du, W. Yue, S. Jiang, Optical fiber SPR biosensor complying with a 3D composite hyperbolic metamaterial and a graphene film, Photon. Res. 9 (3) (2021) 379, https://doi.org/10.1364/prj.416815.

[213] W. Yang, J. Gao, Z. Li, C. Li, Y. Cheng, Y. Huo, S. Jiang, M. Jiang, High performance D-type plastic fiber SPR sensor based on a hyperbolic metamaterial composed of Ag/MgF2, J. Mater. Chem. C 9 (39) (2021) 13647–13658, https://doi.org/10.1039/d1tc02217b.

[214] P. Huo, S. Zhang, Y. Liang, Y. Lu, T. Xu, Hyperbolic metamaterials and metasurfaces fundamentals and applications, Adv. Opt. Mater. 7 (14) (2019) 1801616, https://doi.org/10.1002/adom.201801616.

[215] K.V. Sreekanth, Q. Ouyang, S. Sreejith, S. Zeng, W. Lishu, E. Ilker, W. Dong, M. ElKabbash, Y. Ting, C.T. Lim, M. Hinczewski, G. Strangi, K.T. Yong, R. E. Simpson, R. Singh, Phase-change-material-based low-loss visible-frequency hyperbolic metamaterialsfor ultrasensitive label-free biosensing, Adv. Opt. Mater. 7 (12) (2019) 1–9, https://doi.org/10.1002/adom.201900081.

[216] C.M. Dobson, Protein folding and misfolding, Nature 426 (6968) (2003) 884–890, https://doi.org/10.1038/nature02261.

[217] S.W. Smith, Chiral toxicology it's the same thing. . .only different, Toxicol. Sci. 110 (1) (2009) 4–30, https://doi.org/10.1093/toxsci/kfp097.

[218] E. Hendry, T. Carpy, J.S. Johnston, M. Popland, R. Mikhaylovskiy, A. Lapthorn, S.A. Kelly, L.D. Barron, N. Gadegaard, M. Kadodwala, Ultrasensitive detection and characterization of biomolecules using superchiral fields, Nat. Nanotechnol. 5 (11) (2010) 783–787, https://doi.org/10.1038/nnano.2010.209787.

[219] Y. Zhao, A.N. Askarpour, L. Sun, J. Shi, X. Li, A. Alù, Chirality detection of enantiomers using twisted optical metamaterials, Nat. Commun. 8 (1) (2017), https://doi.org/10.1038/ncomms14180.

[220] R. Tullius, A.S. Karimullah, M. Rodier, B.T. Fitzpatrick, N. Gadegaard, L.D. Barron, V.M. Rotello, G. Cooke, A.J. Lapthorn, M. Kadodwala, "Superchiral" spectroscopy detection of protein higher order hierarchical structure with chiral plasmonic nanostructures, J. Am. Chem. Soc. 137 (26) (2015) 8380–8383, https://doi.org/10.1021/jacs.5b04806.

[221] R. Tullius, G.W. Platt, L.K. Khorashad, N. Gadegaard, A.J. Lapthorn, V.M. Rotello, G. Cooke, L.D. Barron, Z. Wang, A.S. Karimullah, M. Kadodwala, Superchiral plasmonic phase sensitivity for fingerprinting of protein interface structure, ACS Nano 11 (12) (2017) 12049–12056, https://doi.org/10.1021/acsnano.7b04698.

[222] C.B. Kelly, R. Tullius, A.J. Lapthorn, N. Gadegaard, G. Cooke, L.D. Barron, A.S. Karimullah, V.M. Rotello, M. Kadodwala, Chiral plasmonic fields probe structural order of biointerfaces, J. Am. Chem. Soc. 140 (27) (2018) 8509–8517, https://doi.org/10.1021/jacs.8b03634.

[223] G.E. Lio, G. Palermo, R. Caputo, A. De Luca, A comprehensive optical analysis of nanoscale structures from thin films to asymmetric nanocavities, RSC Adv. 9 (37) (2019) 21429–21437, https://doi.org/10.1039/c9ra03684a.

[224] F. Koohyar, A. Rostami, M.J. Chaichi, F. Kiani, Study on thermodynamic properties for binary systems of water + L-cysteine hydrochloride monohydrate, glycerol, and D-sorbitol at various temperatures, J. Chem. (2013) 1–10, https://doi.org/10.1155/2013/601751, 2013.

[225] D.N. Neshev, A.E. Miroshnichenko, Enabling smart vision with metasurfaces, Nat. Photonics 17 (1) (2022) 26–35, https://doi.org/10.1038/s41566-022-01126-4.

[226] E. Wang, D.R. Sell, T. Phan, J.A. Fan, Robust design of topology-optimized metasurfaces, Opt. Mater. Express 9 (2) (2019) 469, https://doi.org/10.1364/ome.9.000469.

[227] J. Wang, Z. Xu, D. Kotsifaki, Plasmonic and metamaterial biosensors A game-changer for virus detection, Sensors & Diagnostics (2023), https://doi.org/10.1039/d2sd00217e.

[228] M. Beruete, I. Jáuregui-López, Terahertz sensing based on metasurfaces, Adv. Opt. Mater. 8 (3) (2020) 1900721, https://doi.org/10.1002/adom.201900721.

[229] X. Chen, H. Park, M. Pelton, X. Piao, N.C. Lindquist, H. Im, Y. Kim, J.S. Ahn, Y.S. Kim, N. Park, D. Kim, S.C. Oh, Atomic layer lithography of wafer-scale nanogap arrays for extreme confinement of electromagnetic waves, Nat. Commun. 4 (1) (2013), https://doi.org/10.1038/ncomms3361.

[230] G.A. López-Muñoz, A. Cortés-Reséndiz, J. Ramón-Azcón, A. Rydosz, Scalable, lithography-free plasmonic metasurfaces by nano-patterned/sculpted thin films for biosensing, Frontiers in Sensors 3 (2022), https://doi.org/10.3389/fsens.2022.945525.

[231] G. Qiu, S. Ng, L.L. Wu, Dielectric functionalization for differential phase detecting localized surface plasmon resonance biosensor, Sensors and Actuators B-chemical 234 (2016) 247–254, https://doi.org/10.1016/j.snb.2016.04.151.
[232] D. Gish, F. Nsiah, M.T. McDermott, M.J. Brett, Localized surface plasmon resonance biosensor using silver nanostructures fabricated by glancing angle deposition, Anal. Chem. 79 (11) (2007) 4228–4232, https://doi.org/10.1021/ac0622274.
[233] A. Thakur, G. Qiu, S. Ng, J. Guan, J. Yue, Y. Lee, C.L. Wu, Direct detection of two different tumor-derived extracellular vesicles by SAM-AuNIs LSPR biosensor, Biosens. Bioelectron. 94 (2017) 400–407, https://doi.org/10.1016/j.bios.2017.03.036.
[234] G. Qiu, S. Ng, C.L. Wu, Bimetallic Au-Ag alloy nanoislands for highly sensitive localized surface plasmon resonance biosensing, Sensors and Actuators B-chemical 265 (2018) 459–467, https://doi.org/10.1016/j.snb.2018.03.066.
[235] A. Nabok, A.G. Al-Rubaye, A.M. Al-Jawdah, A. Tsargorodska, J. Marty, G. Catanante, A. Székács, E. Takacs, [INVITED] Novel optical biosensing technologies for detection of mycotoxins, Opt. Laser Technol. 109 (2019) 212–221, https://doi.org/10.1016/j.optlastec.2018.07.076.
[236] G. Qiu, Y. Yue, J. Tang, Y. Zhao, J. Wang, Total bioaerosol detection by a succinimidyl-ester-functionalized plasmonic biosensor to reveal different characteristics at three locations in Switzerland, Environmental Science & Technology 54 (3) (2020) 1353–1362, https://doi.org/10.1021/acs.est.9b05184.
[237] W. Xu, L. Wang, R. Zhang, X. Sun, L.Q. Huang, H. Su, X. Wei, C. Chen, J. Lou, H. Dai, K. Qian, Diagnosis and prognosis of myocardial infarction on a plasmonic chip, Nat. Commun. 11 (1) (2020), https://doi.org/10.1038/s41467-020-15487-3.
[238] G. Qiu, Z. Gai, L. Saleh, J. Tang, T. Gui, G.A. Kullak-Ublick, J. Wang, Thermoplasmonic-assisted cyclic cleavage amplification for self-validating plasmonic detection of SARS-CoV-2, ACS Nano 15 (4) (2021) 7536–7546, https://doi.org/10.1021/acsnano.1c00957.
[239] N. Kim, M. Choi, J.W. Leem, J.S. Yu, T.Y. Kim, T. Kim, K.M. Byun, Improved biomolecular detection based on a plasmonic nanoporous gold film fabricated by oblique angle deposition, Opt Express 23 (14) (2015) 18777, https://doi.org/10.1364/oe.23.018777.
[240] M. Zandieh, S.A. Hosseini, M. Vossoughi, M. Khatami, S. Abbasian, A. Moshaii, Label-free and simple detection of endotoxins using a sensitive LSPR biosensor based on silver nanocolumns, Anal. Biochem. 548 (2018) 96–101, https://doi.org/10.1016/j.ab.2018.02.023.
[241] K. Sagdic, I. Eş, M. Sitti, F. Inci, Smart materials rational design in biosystems via artificial intelligence, Trends Biotechnol. 40 (8) (2022) 987–1003, https://doi.org/10.1016/j.tibtech.2022.01.005.
[242] J. Wang, Y. Wang, Y. Chen, Inverse design of materials by machine learning, Materials 15 (5) (2022) 1811, https://doi.org/10.3390/ma15051811.
[243] X. Jin, C. Liu, T. Xu, L. Su, X. Zhang, Artificial intelligence biosensors Challenges and prospects, Biosens. Bioelectron. 165 (2020) 112412, https://doi.org/10.1016/j.bios.2020.112412.
[244] F. Faridbod, A.L. Sanati, Graphene quantum dots in electrochemical sensors/biosensors, Curr. Anal. Chem. 15 (2) (2019) 103–123, https://doi.org/10.2174/1573411014666180319145506.
[245] Z.Z. Abidin, Z.Z. Abidin, S.A. Rashid, F.M. Yasin, A.F.M. Noor, M. Issa, Sustainable synthesis processes for carbon dots through response surface methodology and artificial neural network, Processes 7 (10) (2019) 704, https://doi.org/10.3390/pr7100704.
[246] A. Dager, T. Uchida, T. Maekawa, M. Tachibana, Synthesis and characterization of mono-disperse carbon quantum dots from fennel seeds photoluminescence analysis using machine learning, Sci. Rep. 9 (1) (2019), https://doi.org/10.1038/s41598-019-50397-5.
[247] J. Li, T. Chen, K. Lim, L. Chen, S.A. Khan, J. Xie, X. Wang, Deep learning accelerated gold nanocluster synthesis, Advanced Intelligent Systems 1 (3) (2019) 1900029, https://doi.org/10.1002/aisy.201900029.
[248] A.M.R. Gherman, N. Tosa, M.V. Cristea, V. Tosa, S. Porav, P.S. Agachi, Artificial neural networks modeling of the parameterized gold nanoparticles generation through photo-induced process, Mater. Res. Express 5 (8) (2018) 085011, https://doi.org/10.1088/2053-1591/aad0d5.
[249] A.M. Alkilany, S.E. Lohse, C.J. Murphy, The gold standard gold nanoparticle libraries to understand the nano–bio interface, Accounts of Chemical Research 46 (3) (2012) 650–661, https://doi.org/10.1021/ar300015b.
[250] D. Salley, G. Keenan, J. Grizou, A. Sharma, S. Martín, L. Cronin, A nanomaterials discovery robot for the Darwinian evolution of shape programmable gold nanoparticles, Nat. Commun. 11 (1) (2020), https://doi.org/10.1038/s41467-020-16501-4.
[251] G. Moon, J. Choi, C. Lee, Y. Oh, K.H. Kim, D. Kim, Machine learning-based design of meta-plasmonic biosensors with negative index metamaterials, Biosens. Bioelectron. 164 (2020) 112335, https://doi.org/10.1016/j.bios.2020.112335.
[252] Y. LeCun, Y. Bengio, G.E. Hinton, Deep learning, Nature 521 (7553) (2015) 436–444, https://doi.org/10.1038/nature14539.
[253] K. Yao, R. Unni, Y. Zheng, Intelligent nanophotonics merging photonics and artificial intelligence at the nanoscale, Nanophotonics 8 (3) (2019) 339–366, https://doi.org/10.1515/nanoph-2018-0183.
[254] I. Malkiel, M. Mrejen, A. Nagler, U. Arieli, L. Wolf, H. Suchowski, Plasmonic nanostructure design and characterization via Deep Learning, Light Sci. Appl. 7 (1) (2018), https://doi.org/10.1038/s41377-018-0060-7.
[255] Z. Liu, D. Zhu, S.P. Rodrigues, K. Lee, W. Cai, Generative model for the inverse design of metasurfaces, Nano Lett. 18 (10) (2018) 6570–6576, https://doi.org/10.1021/acs.nanolett.8b03171.
[256] W. Ma, F. Cheng, Y. Liu, Deep-learning-enabled on-demand design of chiral metamaterials, ACS Nano 12 (6) (2018) 6326–6334, https://doi.org/10.1021/acsnano.8b03569.
[257] Y. Wu, A. Ray, Q. Wei, A. Feizi, X. Tong, E.E. Chen, Y. Luo, A. Ozcan, Deep learning enables high-throughput analysis of particle-aggregation-based biosensors imaged using holography, ACS Photonics 6 (2) (2019) 294–301, https://doi.org/10.1021/acsphotonics.8b01479.
[258] A. Tittl, A. John-Herpin, A. Leitis, E. Arvelo, H. Altug, Metasurface-based molecular biosensing aided by artificial intelligence, Angew. Chem. 58 (42) (2019) 14810–14822, https://doi.org/10.1002/anie.201901443.
[259] X. Li, J. Shu, W. Gu, L. Gao, Deep neural network for plasmonic sensor modeling, Opt. Mater. Express 9 (9) (2019) 3857, https://doi.org/10.1364/ome.9.003857.
[260] D.N. Neshev, A.E. Miroshnichenko, Enabling smart vision with metasurfaces, Nat. Photonics 17 (1) (2022) 26–35, https://doi.org/10.1038/s41566-022-01126-4.
[261] Z. Li, R. Pestourie, Z. Lin, S.G. Johnson, F. Capasso, Empowering metasurfaces with inverse design principles and applications, ACS Photonics 9 (7) (2022) 2178–2192, https://doi.org/10.1021/acsphotonics.1c01850.
[262] M. Sánchez-Purrà, M. Carré-Camps, H. De Puig, I. Bosch, L. Gehrke, K. Hamad-Schifferli, Surface-enhanced Raman spectroscopy-based sandwich immunoassays for multiplexed detection of Zika and dengue viral biomarkers, ACS Infect. Dis. 3 (10) (2017) 767–776, https://doi.org/10.1021/acsinfecdis.7b00110.
[263] C. Zhang, S. Shen, Q. Wang, M. Lin, Z. Ouyang, Q. Liu, Highly sensitive THz gas-sensor based on the guided bloch surface wave resonance in polymeric photonic crystals, Materials 13 (5) (2020) 1217, https://doi.org/10.3390/ma13051217.
[264] J. Chen, S. Hu, S. Zhu, T. Li, Metamaterials from fundamental physics to intelligent design, Interdisciplinary Materials 2 (1) (2022) 5–29, https://doi.org/10.1002/idm2.12049.